Organic Geochemistry 123 (2018) 74–89

Contents lists available at ScienceDirect

Organic Geochemistry

journal homepage: www.elsevier.com/locate/orggeochem

Thermal alteration of biomarkers in the presence of elemental sulfur and sulfur-bearing minerals during hydrous and anhydrous pyrolysis

Liangliang Wu [a,*], Xinyan Fang [a,b], Shuhuan Ji [a], Ansong Geng [a]

[a] State Key Laboratory of Organic Geochemistry, Guangzhou Institute of Geochemistry, Chinese Academy of Sciences, Wushan, Guangzhou 510640, PR China
[b] University of Chinese Academy of Sciences, Yuquan Road, Beijing 100049, PR China

ARTICLE INFO

Article history:
Received 15 March 2018
Received in revised form 20 June 2018
Accepted 25 June 2018
Available online 25 June 2018

Keywords:
Sulfur alteration of biomarker
Biomarker concentration
Biomarker distribution

ABSTRACT

Although elemental sulfur and sulfur-bearing minerals are not the main constituents of sedimentary rock, they are still important for the formation and destruction of biomarkers. In this study, a bitumen of Sichuan Basin mudstone with abundant biomarkers was separately pyrolyzed (under both hydrous and anhydrous conditions) with elemental sulfur (S^0) and sulfur-bearing minerals (including pyrite, ferrous sulfate, and ferric sulfate) at various temperatures (300, 330 and 350 °C). The results show that the effects of different forms of sulfur on the evolution of biomarkers vary. Pyrite (FeS_2) had only a slight influence on the characteristics of the biomarkers during anhydrous and hydrous pyrolysis. On the other hand, the presence of S^0, ferrous sulfate ($FeSO_4$) and ferric sulfate ($Fe_2(SO_4)_3$) promoted the thermal cracking of the biomarkers and changed the biomarker distributions under anhydrous conditions. The extent of biomarker thermal alterations decreased in the following order: $S^0 > Fe_2(SO_4)_3 > FeSO_4 > FeS_2$. Additionally, the presence of water seemed to promote the effects of the sulfur additive on the changes in biomarker compositions, but this did not change their raking in terms of influence. The elemental sulfur alteration of the biomarkers increased with pyrolysis temperature (simulated maturity) and the abundance of elemental sulfur in the sample. The results obtained offer new insights into how biomarkers evolve when elemental sulfur and sulfur-bearing minerals are present.

1. Introduction

Sulfur and sulfur-bearing minerals widely occur in marine source rocks (Acholla and Orr, 1993; Jensen et al., 1998; Chen et al., 2000; Zopfi et al., 2004; Zhang et al., 2011; Berthonneau et al., 2016; Cai et al., 2017; Rosenberg et al., 2017) due to the abundance of SO_4^{2-} in seawater. FeS_2 (pyrite) is considered to be the most abundant reduced sulfur species and serves as a long-term sink for sulfur in most continental margin sediments (Goldhaber and Kaplan, 1975; Berner, 1989; Riedinger et al., 2017). Jensen et al. (1998) reported that the relative abundance of mineral sulfur (mainly pyrite) normalized to TOC for 43 source rocks (43 samples with sulfur-bearing minerals among 56 samples) was within the range 0.1–146% with an average value of 20.8%. Kelemen et al. (2007) reported that sulfate was the dominant form of sulfur in 18 kerogens (representing several major petroleum source facies). Sulfur and sulfur-bearing minerals (such as pyrite, sphalerite, and galena) have also been widely reported in some deep, hot carbonate reservoir rocks (e.g., Krouse et al., 1988; Sassen, 1988; Cai et al., 2003, 2004; Zou et al., 2008; Zhu et al., 2011).

Although sulfur and sulfur-bearing minerals are minor constituents of most sediments, they may still significantly influence the thermal evolution of organic matter (OM) in sediments and petroleum reservoirs. Reactions occurring between S^0 (elemental sulfur) and OM may lead to sulfur incorporation (Kowalewski et al., 2010), the formation of unsaturated organic compounds (e.g., aromatics) from alicyclic saturated hydrocarbons (Toland et al., 1958; Abbott et al., 1985; White et al., 1988), and the degradation of biomarkers (Abbott et al., 1985; Comet et al., 1986). Lu et al. (2012) reported that the pyrolysis of pure *n*-C_{24} with S^0 produce alkenes and H_2S because S radicals have a high affinity for H abstraction. Aqueous sulfates mainly influence petroleum reservoirs through thermochemical sulfate reduction (TSR), which has been widely studied by previous researchers (e.g., Orr, 1974; Machel et al., 1995; Worden et al., 1995; Meshoulam et al., 2016). The TSR process involves oxidation of hydrocarbons in reservoirs by inorganic aqueous sulfate, with CO_2 and H_2S products typically generated (Orr, 1974; Machel et al., 1995; Worden et al.,

* Corresponding author.
E-mail address: wuliangliang@gig.ac.cn (L. Wu).

https://doi.org/10.1016/j.orggeochem.2018.06.010
0146-6380/

1995). Sulfides from assimilatory SO_4^{2-} reduction can also be incorporated into OM (i.e., S_{org}: organic sulfur) though sulfurization processes (Francois, 1987). Pyrite is also considered to have a catalytic effect on the pyrolysis behavior of coal (e.g., Lambert Jr., 1982; Thomas et al., 1982; Bakr et al., 1991; Metecan et al., 1999) and oil shale (Garg and Givens, 1982; Chen et al., 2000).

The influence and reaction mechanisms of sulfur and sulfur-bearing minerals on the generation and evolution of OM is generally well understood. Most reactions between S-species (sulfur-containing species) and OM can be attributed to free-radical mechanisms (Lewan, 1998). S^0 likely enables free radicals to promote the thermal cracking of C—C bonds to occur at a faster rate and at a lower stage of thermal maturity (Abbott et al., 1985; Lewan, 1998). Recently, an experiment conducted by Said-Ahmad et al. (2013) showed that water can also promote the oxidation of OM when elemental sulfur is present. The pyrolysis behavior of oil shale has also been related to pyrite decomposition (Gai et al., 2014). The S^0 that is released from pyrite can hasten the degradation of OM. However, radical mechanisms are not likely to be dominant in the initial stages of thermochemical sulfate reduction (TSR), which involves the reduction of sulfate to sulfide coupled with the oxidation of hydrocarbons (Worden et al., 1995). Recently, a revised two-stage reaction scheme was proposed to explain the mechanisms of TSR (Amrani et al., 2008; Zhang et al., 2008, 2012; Meshoulam et al., 2016). This model suggests that the first stage involves a slow process of HSO_4^- reduction and the second stage involves H_2S-catalyzed reactions (carbonium ion mechanisms). The H_2S reacts with hydrocarbons to form labile organic compounds (which may be separately released through the cracking of bitumen) that in turn catalyze the TSR (Amrani et al., 2008; Zhang et al., 2008).

The roles of sulfur and sulfur-bearing minerals in the generation and evolution of sedimentary organic matter (OM) have been of interest to organic geochemists for decades. However, most previous studies have focused on the pyrolysis behaviors of fossil fuels or single organic compounds in the presence of S-species. Few studies have looked at their effects on specific biomarkers in crude oils and/or sedimentary organic matter that persist due to their stable structures. Biomarkers are widely used in oil studies to help evaluate thermal maturity assessments, organofacies studies, and oil–oil/oil–source rock correlations (Peters et al., 2005 and References therein) and the degrees of oil source mixings (e.g., van Aarssen et al., 1999; Jiang and Li, 2002; Zhan et al., 2016). Understanding the interacting effects of organic matter inputs, mineral composition, and thermal maturity on the evolution of biomarkers is important to most geochemical evaluations (Tissot and Welte, 1984; Price, 1993; Koopmans et al., 1998; Peters et al., 2005; Pan et al., 2010). However, few studies have reported the influence of S-species on biomarkers (Abbott et al., 1985; Comet et al., 1986). Currently, we still know little about the extent to which elemental sulfur and sulfur-bearing minerals in source rocks affect the evolution of biomarkers.

The aim of this study was to investigate the influence of S-species commonly found in natural source rocks (including elemental sulfur, pyrite, ferrous sulfate, and ferric sulfate) on the thermal evolution of biomarkers. Bitumen, rather than kerogen extracted from the Dalong Formation source rock, was used because it can be isolated from co-occurring S-species. Elemental sulfur and sulfur-bearing minerals are difficult to remove from the kerogen fraction. In this study, the hydrous and anhydrous pyrolysis of bitumen combined with different forms of sulfur, including elemental sulfur and three sulfur-bearing minerals (pyrite, ferrous sulfate, and ferric sulfate) was conducted and biomarkers quantitatively analysed to examine the effects of S-species on their evolution.

2. Samples and methods

2.1. Samples

The bitumen sample investigated in this study was extracted from the Permian Dalong Formation mudstone (GY-8) in the Sichuan Basin, China (Lat. 32° 19′ 11″ N, Long. 105° 27′ 18″ E). The basic geochemical characteristics of sample GY-8 have already been presented by Wu et al. (2012, 2013) and Wu and Geng (2016). The investigated sample is classified as an early mature Type II kerogen with total organic carbon (TOC) levels of 8.76% and a % Ro (vitrinite reflectance) value of 0.58. The distributions of biomarkers found in the original bitumen of GY-8 are shown in Fig. 1, with assignments listed in Table 1. First, GY-8 mudstone was powdered into 80–100 mesh. Then, the source rock powder was extracted by a mixture of DCM (dichloromethane) and methanol (93:7, v/v), with excess copper turnings added to the Soxhlet apparatus to remove the extracted elemental sulfur. Thus, all elemental sulfur that existed in the extracted bitumen was removed.

2.2. Pyrolysis experiments

In this study, all pyrolysis experiments were conducted using glass tubes, and both hydrous and anhydrous pyrolysis conditions were used. First, the pure bitumen or bitumen (roughly 50 mg) combined with finely ground additives, were placed into the glass tubes (20 mm o.d., 1 mm wall thickness, 100 mm length and ca. 25 mL volume). Pure water (de-ionized water:bitumen, 1:2, w/w) was also added to the glass tubes for the hydrous pyrolysis experiments. The tubes were sealed under vacuum conditions for pyrolysis experiments. The additives used were elemental sulfur (S^0) or one of three sulfur-bearing minerals: ferrous disulfide (FeS_2), ferrous sulfate ($FeSO_4$), and ferric sulfate ($Fe_2(SO_4)_3$). Elemental sulfur (S^0 > 99.5%), pyrite (FeS_2 > 99.8%), ferrous sulfate heptahydrate ($FeSO_4{\cdot}7H_2O$ > 99.0%) and ferric sulfate hydrate ($Fe_2(SO_4)_3{\cdot}xH_2O$, Fe: 21–23%) were purchased from Sigma-Aldrich. The $FeSO_4$ and $Fe_2(SO_4)_3$ were obtained by heating $FeSO_4{\cdot}7H_2O$ and $Fe_2(SO_4)_3{\cdot}xH_2O$ in a vacuum oven at 200 °C for 4 h. The S^0 and FeS_2 were used without further purification. Then, three series of pyrolysis experiments were conducted at temperatures of 300 °C, 330 °C, and 350 °C. The calculated vitrinite reflectance from the Easy %Ro method (Sweeney and Burnham, 1990) for the bitumen that was heated to 300 °C, 330 °C, and 350 °C for 72 h were 0.70%, 0.87%, and 1.07%, respectively. A relative abundance of 20% for the different additives was used at 300 °C and 330 °C, while a relative abundance of S^0 in the range from 20% to 100% was used for the experiments at 350 °C. The vessels were heated to the desired temperature within 2 h, and were then held isothermally for 72 h. The conditions for each pyrolysis experiment are shown in Table 2. Meanwhile, pyrolysis of bitumen alone (without sulfur-bearing compounds) was also conducted and to compare to the pyrolysis of bitumen with different additives.

After pyrolysis, the tubes were cracked and the pyrolysates (pyrolysis products) were recovered by repeated sonication with a mixture of DCM and methanol (93:7, v/v). Gaseous products were not directly measured. However, the absolute amount of low molecular weight compounds (LMW, carbon number < 14, including gaseous products) was calculated by mass balance. Asphaltenes were precipitated from the products by adding 50-fold (volume ratio for *n*-hexane/bitumen) cold *n*-hexane and were then removed by centrifugation. The maltene fractions were then fractionated by silica/alumina (3:1, v/v) column chromatography into saturated, aromatic and polar fractions by elution with *n*-hexane, DCM/*n*-hexane (3:1, v/v) and DCM/methanol (2:1, v/v), respectively. Internal standards, D_4C_{27} 5α-cholane and $C_{12}D_8S$ dibenzothiophene,

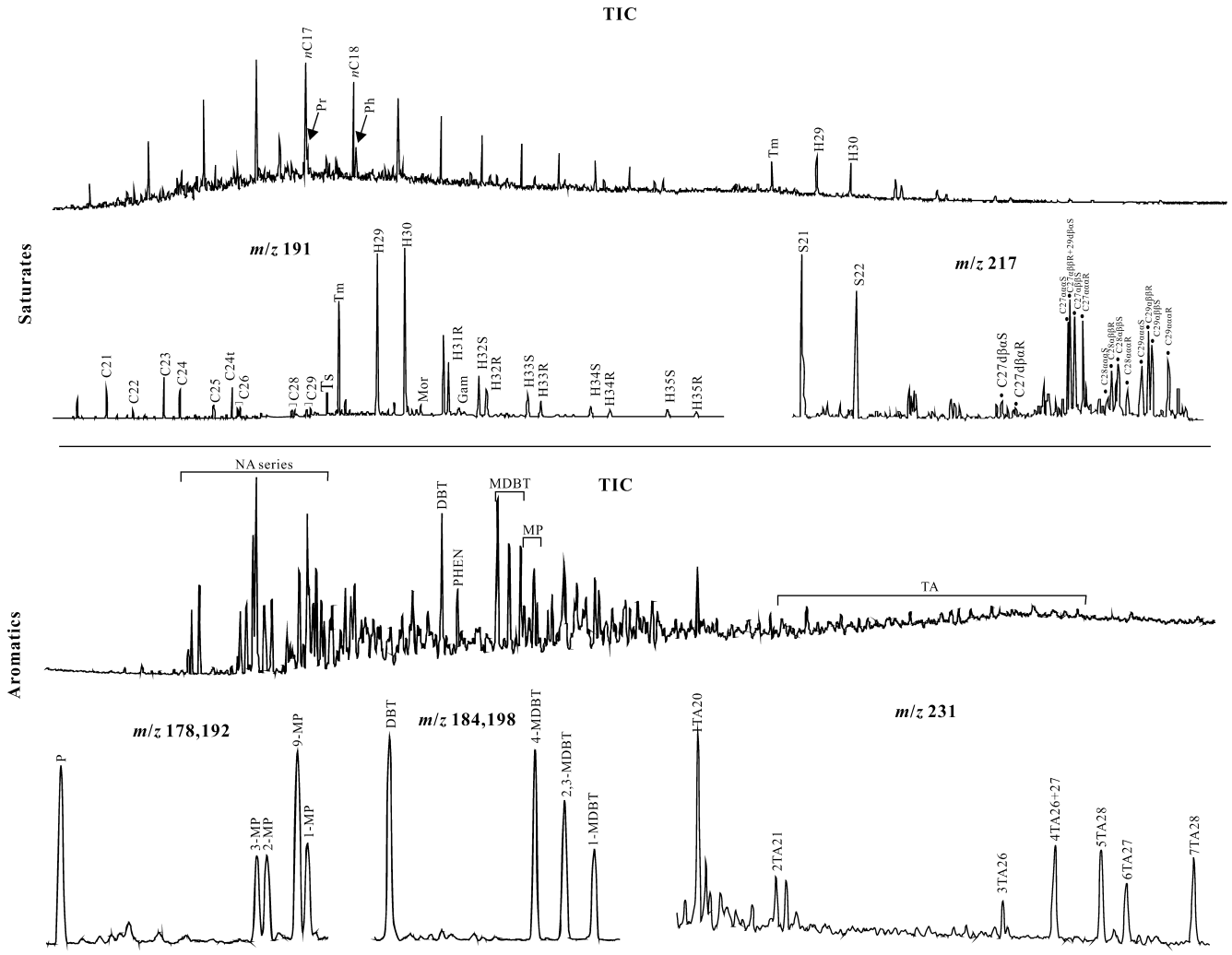

Fig. 1. The characteristics of biomarkers in the original bitumen of GY-8. The peak assignments are listed in Table 1.

were injected into saturated and aromatic hydrocarbon fractions, respectively, to determine the absolute biomarker concentration.

2.3. GC–MS analysis

The saturated biomarkers were analyzed using a Thermo Scientific Trace GC Ultra gas chromatograph coupled to a Thermo Scientific Trace DSQ II mass spectrometer. A DB-1 fused silica capillary column (60 m × 0.32 mm i.d. × 0.25 μm film thickness) was used. The GC oven was set at 70 °C for 2 min and was then programmed to 290 °C at 4 °C/min, with a final hold time of 30 min. The aromatic hydrocarbon fraction was analyzed by the same GC–MS with the same GC column, and the temperature program was held isothermally at 70 °C for 2 min, programmed to 140 °C at 6 °C/min, and then to 290 °C at 3 °C/min with a final hold time of 25 min. Helium was used as a carrier gas with a constant flow rate of 1.5 mL/min. The ion source temperature was set to 250 °C, and the temperature of the injector was set to 290 °C. The ion source was operated in the electron impact (EI) mode with an electron energy level of 70 eV. The GC–MS analyses were carried out in selected ion monitoring mode (SIM). The selected ions that were monitored included *m*/*z* 191 (terpanes) and *m*/*z* 217 (steranes).

The tricyclic terpane biomarkers investigated in this study included C_{21}–C_{29}, with C_{26}, C_{28}, and C_{29} compounds having two-isomer pairs. A C_{24} tetracyclic terpane peak was also evaluated. The hopane biomarkers that were used included C_{29} 17β-norhopane, C_{30} 17β(H)-hopane, homohopanes (H31 to H35 pairs), C_{30} moretane, C_{27} 17α(H)-22,29,30-trisnorhopane (Tm), C_{27} 18α(H)-22,29,30-trisnorneohopane (Ts) and gammacerane. The sterane biomarkers consisted of C_{21}, C_{22}, C_{27} dia and C_{27}–C_{29} steranes with four stereoisomers (5α,14α,17α(H)-20S; 5α,14β,17β(H)-20R; 5α,14α,17α(H)-20S; 5α,14α,17α(H)-20R). The triaromatic steroidal hydrocarbons included C_{20}, C_{21} and C_{26}–C_{28} homologues. The relative standard deviation (RSD) for most biomarker quantitative analysis was <10%, based on 5 duplicate experiments (Tables 3 and 5).

3. Results and discussion

3.1. The influence of different types of sulfur on bulk compositions (SARA fractions)

Fig. 2 compares the relative abundances of low molecular weight hydrocarbons (LMW, including gas and C_6–C_{14}), saturates, aromatics, resin and asphaltene fractions for all pyrolysis experiments. It is clear that the distribution of the SARA fractions for pyrolysates with different additives vary under the same pyrolysis conditions. Generally speaking, thermal alteration cracks the high molecular weight hydrocarbons (HMW) into LMW hydrocarbons. The yields of LMW pyrolysates obtained with the additives are

Table 1
Biomarker identifications.

Abbreviations	Biomarker names	Abbreviations	Biomarker names
Terpanes		C27αββR+29dβαS	C_{27}-5α,14β,17β,20R-cholestane+C_{29}-13β,17α,20S-diastigmastane
C21	C_{21}-tricyclic terpane	C27αββS	C_{27}-5α,14β,17β,20S-cholestane
C22	C_{22}-tricyclic terpane	C27αααR	C_{27}-5α,14α,17α,20R-cholestane
C23	C_{23}-tricyclic terpane	C28αααS	C_{28}-5α,14α,17α,20S-ergostane
C24	C_{24}-tricyclic terpane	C28αββR	C_{28}-5α,14β,17β,20R-ergostane
C25	C_{25}-tricyclic terpane	C28αββS	C_{28}-5α,14β,17β,20S-ergostane
C24t	C_{24}-tetracylic terpane	C28αααR	C_{28}-5α,14α,17α,20R-ergostane
C26R	C_{26}-R tricyclic terpane	C29αααS	C_{29}-5α,14α,17α,20S-stigmastane
C26S	C_{26}-S tricyclic terpane	C29αββR	C_{29}-5α,14β,17β,20R-stigmastane
C28R	C_{28}-R tricyclic terpane	C29αββS	C_{29}-5α,14β,17β,20S-stigmastane
C28S	C_{28}-S tricyclic terpane	C29αααR	C_{29}-5α,14α,17α,20R-stigmastane
C29R	C_{29}-R tricyclic terpane	*Phenanthrenes*	
C29S	C_{29}-S tricyclic terpane	PHEN	Phenanthrene
Hopanes		3-MP	3-Methylphenanthrene
Ts	C_{27}-18α-22,29,30-trisnorneohopane	2-MP	2-Methylphenanthrene
Tm	C_{27}-17α-22,29,30-trisnorhopane	9-MP	9-Methylphenanthrene
H29	C_{29}-17α(H),21β(H)-hopane	1-MP	1-Methylphenanthrene
H30	C_{30}-17α(H),21β(H)-hopane	*Dibenzothiophenes*	
Mor		DBT	Dibenzothiophene
H31S	C_{31}-17α(H),21β(H),22S-hopane	4-MDBT	4-Methyldibenzothiophene
H31R	C_{31}-17α(H),21β(H),22R-hopane	2,3-MDBT	3,2-Methyldibenzothiophene
Gam	Gammacerane	1-MDBT	1-Methyldibenzothiophene
H32S	C_{32}-17α(H),21β(H),22S-hopane	*Triaromatic Steranes*	
H32R	C_{32}-17α(H),21β(H),22R-hopane	1TA20	C_{20}-Triaromatic Sterane
H33S	C_{33}-17α(H),21β(H),22S-hopane	2TA21	C_{21}-Triaromatic Sterane
H33R	C_{33}-17α(H),21β(H),22R-hopane	3TA26	C_{26}-Triaromatic Sterane (20S)
H34S	C_{34}-17α(H),21β(H),22S-hopane	4TA26 + 27	C_{26}-Triaromatic Sterane (20R)+C_{27}-Triaromatic Sterane (20S)
H34R	C_{34}-17α(H),21β(H),22R-hopane	5TA28	C_{28}-Triaromatic Sterane (20S)
H35S	C_{35}-17α(H),21β(H),22S-hopane	6TA27	C_{27}-Triaromatic Sterane (20R)
H35R	C_{35}-17α(H),21β(H),22R-hopane	7TA28	C_{28}-Triaromatic Sterane (20R)
Steranes		*Others*	
S21	5α,14β,17β(H)-pregnane (diginane)	nC17	C_{17} *n*-alkane
S22	5α,14β,17β(H)-homopregnane (20-methyldiginane)	Pr	Pristane
C27dβαS	C_{27}-13β,17α,20S-diacholestane	nC18	C_{18} *n*-alkane
C27dβαR	C_{27}-13β,17α,20R-diacholestane	Ph	Phytane
C27αααS	C27-5α,14α,17α,20S-cholestane		

Table 2
Conditions used in the pyrolysis experiments.

No.	Temp (°C)	Weight of additive/weight of bitumen (%)				
		FeS_2	$FeSO_4$	$Fe_2(SO_4)_3$	S	H_2O
1	300	0	0	0	0	0
2	300	20	0	0	0	0
3	300	0	20	0	0	0
4	300	0	0	20	0	0
5	300	0	0	0	20	0
6	330	0	0	0	0	0
7	330	20	0	0	0	0
8	330	0	20	0	0	0
9	330	0	0	20	0	0
10	330	0	0	0	20	0
11	350	0	0	0	20	0
12	350	0	0	0	50	0
13	350	0	0	0	100	0
14	350	0	0	0	0	0
15	300	0	0	0	0	50
16	300	20	0	0	0	50
17	300	0	20	0	0	50
18	300	0	0	20	0	50
19	300	0	0	0	20	50
20	330	0	0	0	0	50
21	330	20	0	0	0	50
22	330	0	20	0	0	50
23	330	0	0	20	0	50
24	330	0	0	0	20	50

different from that obtained with bitumen alone under the same pyrolysis conditions. This demonstrates that the presence of different forms of sulfur indeed had a catalytic effect on the thermal alteration of the hydrocarbons. Taking anhydrous pyrolysis at 330 °C as an example, the pyrolysis of bitumen alone only generated a small amount LMW hydrocarbon (9%) while the pyrolysis of bitumen with FeS_2, $FeSO_4$, $Fe_2(SO_4)_3$ and S^0 converted approximately 15%, 24%, 40% and 63% of the bitumen into LMW hydrocarbons, respectively (Table 3, Fig. 2B). These results indicate that the effects of different forms of sulfur on the thermal degradation of bitumen followed the order: $S^0 > Fe_2(SO_4)_3 > FeSO_4 > FeS_2$. The presence of water seemed to slightly promote the effects of different forms of sulfur on the evolution of biomarkers at 330 °C, but this did not change their ranking.

In natural settings, the onset temperature required to initiate TSR ranges from 100 °C to 140 °C, while it generally exceeds 200 °C under most laboratory conditions (Toland, 1960; Kiyosu and Krouse, 1993; Cross et al., 2004; Xia et al., 2014). In this study, the ≥300 °C pyrolysis temperatures were sufficient to initiate TSR reactions. The TSR oxidizes hydrocarbons in reservoirs by inorganic aqueous sulfate, with CO_2 and H_2S as the primary products (Orr, 1974; Machel et al., 1995; Worden et al., 1995). Although the yields of H_2S derived from each experiment were not specially measured, high yields of LMW hydrocarbons (including H_2S gas evident from its familiar odour) generated from the hydrous and anhydrous experiments involving $Fe_2(SO_4)_3$ and $FeSO_4$ (relative to the experiment involving bitumen alone) demonstrated that TSR occurred.

The presence of ferrous and ferric sulfate also affects bitumen even during anhydrous pyrolysis at 300 °C and 330 °C. This result is consistent with the report by Heydari and Moore (1989), who claimed that solid anhydrite is reduced during TSR in natural conditions. In observing the replacement of solid sulfate with calcite (Heydari and Moore, 1989), they found that the degradation of OM by anhydrous sulfate likely occurs due to the thermochemical

Table 3
The relative abundance of SARA fractions and LMW fraction.

Temp (°C)	Run No.	Conditions	Relative abundance (%)				
			LMW	Saturated	Aromatic	Resin	Asphaltene
Anhydrous pyrolysis							
300	1	–	0.6	9.7	13.4	13.3	63.1
300	2	FeS_2	0.2	10.6	12.6	10.8	65.8
300	3	$FeSO_4$	12.9	9.2	12.4	8.8	56.8
300	4	$Fe_2(SO_4)_3$	40.8	9.6	8.6	5.6	35.4
300	5	S (20%)	57.1	7.9	8.1	4.7	22.2
330	6	–	9.1	12.9	11.7	8.5	57.8
330	7	FeS_2	14.7	10.3	12.1	8.7	54.2
330	8	$FeSO_4$	23.9	11.4	11.2	6.7	47.5
330	9	$Fe_2(SO_4)_3$	39.6	9.8	6.5	5.5	38.6
330	10	S (20%)	62.6	6.4	4.5	3.4	23.0
350	11	–	24.7	14.9	12.5	7.6	40.3
350	12	S (20%)	63.9	8.9	5.2	3.1	18.9
350	13	S (50%)	94.8	2.8	0.8	1.2	0.4
350	14	S (100%)	97.1	1.8	0.4	0.4	0.4
Hydrous pyrolysis							
300	15	–	5.5	12.1	21.8	11.6	49.0
300	16	FeS_2	1.2	12.3	24.8	10.7	50.9
300	17	$FeSO_4$	11.1	10.6	22.1	9.6	46.6
300	18	$Fe_2(SO_4)_3$	29.3	5.4	10.6	11.0	43.7
300	19	S (20%)	56.0	3.1	4.1	4.7	32.2
330	20	–	18	3.0	15.8	25.6	37.6
330	21	FeS_2	20.9	3.9	16.0	22.7	37.5
330	22	$FeSO_4$	24.7	3.7	13.0	10.2	48.4
330	23	$Fe_2(SO_4)_3$	72.1	1.2	6.1	4.7	15.9
330	24	S (20%)	64.6	6.5	6.5	4.4	18.1

Note: LMW (including gas and C_{6-14}) = total bitumen – asphaltene – maltene.

breakdown of solid sulfate as shown by reaction Eq. (1) (Siebert, 1985). The formed S^0 can subsequently alter OM. Meanwhile, trace amounts of water generated from the bitumen or found in sulfate minerals might contribute to partial anhydrous pyrolysis.

$$CaSO_4+3H_2S+CO_2 \rightarrow CaCO_3+4S^0+3H_2O \quad (1)$$

Sulfur radical mechanisms can be used to explain reactions involving S^0 (Abbott et al., 1985; Lewan, 1998). The minimum reaction temperature required for the cleavage of the cyclo-S_8 allotrope (the most prevalent form of S^0 found in nature) is approximately 175 °C (Goldstein and Aizenshtat, 1994). Above this temperature, sulfur in cyclic S_8 opens to form a highly reactive polysulfide diradical, which is the active species involved in hydrogen abstraction from organic compounds (Abbott et al., 1985; Goldstein and Aizenshtat, 1994). Water also contributes to the reaction of sulfur with OM (Said-Ahmad et al., 2013). The hydrolysis of sulfur is favorable at temperatures exceeding 150 °C (Goldstein and Aizenshtat, 1994), which is lower than the temperature required for sulfur cleavage under anhydrous conditions.

Through the formation of S^0, pyrite can affect the pyrolysis behavior of OM (Bakr et al., 1991; Gai et al., 2014). The formed S^0 subsequently destroys OM through the processes described above. Thus, the main factor that controls the degradation of OM by pyrite is its decomposition. The activation temperature required for the decomposition of pyrite under anhydrous conditions is approximately 500–530 °C (Chen et al., 2000; Gai et al., 2014). Hydrogen donors in coal were shown to reduce the decomposition temperature of pyrite by approximately 100 °C (Chen et al., 2000). Moreover, pyrite presents different levels of thermal stability in the presence or absence of water. The decomposition of pyrite under hydrous conditions occurs between 440 °C and 560 °C (Levy and White, 1988). Hydrous pyrolysis of pyrite at 350 °C for 72 h by Ding and Liu (2017) detected no H_2S. As temperatures used in this study (300–330 °C) were lower than the minimal decomposition temperature of pyrite, the effects of pyrite on the thermal alteration of the bitumen were minor (Fig. 2).

3.2. The influence of different forms of sulfur on biomarker concentrations

The absolute concentrations of individual biomarkers were measured to investigate the evolution of biomarkers with the addition of different additives at various conditions (temperature; the presence of water). A relative abundance variation ratio (RAVR) was developed by Chen et al. (2016) to reflect the changes in biomarker concentrations observed at different temperatures. We used a modified RAVR to reflect the effects of different additives on individual biomarker concentrations. When the absolute abundance of an individual biomarker used in the experiment of bitumen with a certain additive was *a*, that for the experiment on bitumen alone at the same temperature was *b*, and the RAVR for this additive was calculated as $(a–b)/b \times 100\%$. The positive RAVR values for a certain additive show that corresponding additive will prohibit the degradation of biomarkers or promote the generation of biomarkers, while negative RAVR values for a certain additive indicate that such an additive promotes the degradation of biomarkers. Pyrolysis experiments (330 °C for four weeks) conducted by Mango (1990) reported the decomposition ratios of cholestane and octadecane were 17% and 2.3% respectively, indicating that the pyrolysis behaviors for different biomarkers can vary considerably. Thus, terpane, sterane, and triaromatic steroid hydrocarbons are separately discussed.

3.2.1. Terpanes

Several classes of terpanes in petroleum originate from bacterial (prokaryotic) membrane lipids (Ourisson et al., 1982). Tricyclic terpanes and pentacyclic triterpanes (hopanes) are the two most commonly used classes of terpanes.

Similar concentrations of individual tricyclic terpane were detected from all 300 °C anhydrous pyrolysis experiments (Table 4), and their RAVR values with S-additives were all <−25% (Fig. 3A). The additives had a stronger effect on hopanes (Fig. 3E), consistent with the higher thermal stabilities of tricyclic and

Table 4
Absolute concentrations (μg/g) of each saturate biomarker from the pyrolysates of bitumen with various additives at different temperatures.

Biomarkers	300 °C										330 °C										350 °C			
	Anhydrous					Hydrous					Anhydrous					Hydrous					Anhydrous			
	N	S20	Fe1	Fe2	Fe3	N	S20	Fe1	Fe2	Fe3	N	S20	Fe1	Fe2	Fe3	N	S20	Fe1	Fe2	Fe3	N	S20	S50	S100
Terpanes																								
C21	24.8	20.9	27.1	27.1	24.1	32.3	12.5	32.7	28.7 ± 1.2	14.0	25.8 ± 0.4	8.9	26.7	25.5 ± 1.5	21.8	28.9 ± 1.9	–	28.7	13.2 ± 1.1	–	23.6	6.1	–	–
C22	7.1	5.4	9.6	7.8	6.5	41.9	17.2	42.0	40.4 ± 2.1	22.1	7.1 ± 0.2	2.0	6.7	7.3 ± 0.3	5.5	36.8 ± 2.7	–	38.3	19.1 ± 2.9	–	6.8	1.7	–	–
C23	32.8	25.7	33.5	32.7	30.3	59.5	23.7	50.7	49.6 ± 0.8	31.5	29.8 ± 2.6	9.4	29.5	26.6 ± 1.4	24.1	46.3 ± 3.2	–	48.6	19.9 ± 3.7	–	28.7	5.8	–	–
C24	22.8	16.4	22.6	22.4	20.8	39.8	12.4	38.8	33.7 ± 1.3	19.9	21.2 ± 1.6	5.8	18.5	16.8 ± 1.6	15.5	29.8 ± 2.0	–	31.2	18.1 ± 1.1	–	19.4	3.4	–	–
C25	20.6	13.9	19.4	18.4	17.3	31.0	8.8	32.7	26.2 ± 1.7	13.7	15.4 ± 0.6	4.9	14.9	11.6 ± 0.7	11.7	24.3 ± 1.4	–	23.6	10.3 ± 1.8	–	14.7	2.8	–	–
C24t	20.2	19.6	19.8	20.1	17.5	21.9	8.4	20.9	20.2 ± 0.9	11.5	15.5 ± 0.7	9.4	15.0	12.4 ± 1.1	13.4	23.6 ± 1.8	–	25.3	13.4 ± 1.1	–	16.0	6.0	–	–
C26R	7.8	4.6	6.2	6.8	6.1	19.5	4.8	17.8	6.4 ± 0.2	5.4	5.8 ± 0.3	1.4	4.8	3.8 ± 0.4	4.3	10.3 ± 0.8	–	11.7	4.0 ± 0.9	–	5.7	0.7	–	–
C26S	6.8	4.8	5.6	5.6	6.3	17.8	4.6	16.4	5.7 ± 0.1	5.1	5.4 ± 0.4	1.4	5.2	3.8 ± 0.5	4.7	10.1 ± 0.3	–	11.3	4.0 ± 0.7	–	5.7	0.7	–	–
C28R	5.5	4.3	4.5	5.6	5.8	9.8	2.4	6.9	5.1 ± 0.2	1.5	3.8 ± 0.2	1.7	4.4	3.7 ± 0.1	3.8	6.8 ± 0.3	–	5.4	3.2 ± 0.2	–	4.2	0.9	–	–
C28S	5.4	3.4	4.1	5.9	5.6	5.7	2.7	7.6	4.4 ± 0.4	1.3	4.9 ± 0.1	1.5	4.2	3.8 ± 0.3	4.0	6.8 ± 0.4	–	6.0	3.2 ± 0.2	–	4.0	1.1	–	–
C29R	7.3	6.3	7.1	6.5	6.1	5.7	1.3	6.3	4.6 ± 0.3	1.5	4.7 ± 0.2	1.6	6.6	4.2 ± 0.4	5.9	7.9 ± 0.5	–	6.2	2.0 ± 0.1	–	6.7	0.6	–	–
C29S	5.8	4.1	6.1	4.8	4.9	7.5	1.3	6.9	5.7 ± 0.1	3.5	4.6 ± 0.2	1.9	4.9	3.9 ± 0.2	3.6	8.2 ± 0.1	–	6.7	1.8 ± 0.2	–	4.7	0.6	–	–
Total	167.1	129.3	165.6	163.7	151.4	292.4	100.3	278.9	230.7	130.9	143.4	50.0	141.4	123.4	118.3	239.8	0.0	243.0	112.2	0.0	140.1	30.3	–	–
Hopanes																								
Ts	18.7	13.2	14.7	15.0	12.7	30.8	11.6	32.7	27.6 ± 1.3	8.4	11.8 ± 0.3	5.5	10.9	6.9 ± 0.8	10.3	21.9 ± 1.9	–	23.5	9.7 ± 1.4	–	11.0	2.8	–	–
Tm	84.6	53.6	78.3	68.7	59.6	130.3	25.7	132.2	116.9 ± 4.5	30.4	49.8 ± 4.1	16.7	53.9	39.3 ± 3.4	39.3	118.9 ± 3.7	–	125.2	40.3 ± 4.0	–	42.8	6.4	–	–
H29	137.2	82.9	134.0	107.6	102.3	217.4	34.3	213.9	189.8 ± 11.8	41.3	87.2 ± 5.1	23.6	88.9	58.9 ± 3.1	57.9	179.3 ± 16.9	–	194.5	62.7 ± 12.9	–	76.7	6.9	–	–
H30	152.2	85.8	146.1	124.6	114.1	223.2	32.6	228.5	207.5 ± 5.2	39.9	82.7 ± 2.6	21.5	83.3	57.0 ± 6.7	53.1	189.6 ± 8.1	–	199.8	61.1 ± 9.7	–	60.6	5.2	–	–
Mor	12.3	8.5	9.9	11.4	6.8	12.9	3.9	14.0	10.8 ± 0.5	5.6	6.5 ± 0.5	2.2	6.5	4.2 ± 0.2	3.8	13.1 ± 0.9	–	17.8	5.2 ± 1.3	–	6.2	–	–	–
H31S	74.9	40.4	71.0	58.0	49.8	115.0	12.7	119.0	106.1 ± 3.1	13.2	38.1 ± 2.7	9.5	39.9	28.5 ± 1.5	24.6	86.5 ± 4.6	–	63.4	34.8 ± 2.3	–	29.8	–	–	–
H31R	52.7	33.9	52.8	42.4	38.9	70.7	8.6	77.3	66.8 ± 4.0	8.6	33.1 ± 1.3	9.1	31.7	20.5 ± 1.9	22.1	54.9 ± 4.3	–	39.4	19.1 ± 2.4	–	19.2	–	–	–
Gam	3.8	4.1	4.8	3.5	4.2	19.1	3.8	13.6	10.4 ± 0.6	3.2	2.6 ± 0.2	0.9	2.5	3.2 ± 0.1	1.7	11.8 ± 0.7	–	23.8	4.9 ± 1.4	–	2.4	–	–	–
H32S	37.9	22.6	40.5	33.3	26.5	59.1	5.4	63.0	53.5 ± 6.3	8.0	23.1 ± 0.9	5.4	23.5	16.6 ± 1.4	12.7	48.4 ± 1.1	–	38.1	20.3 ± 1.2	–	15.6	–	–	–
H32R	28.3	18.0	27.4	22.6	18.9	46.1	4.5	42.1	40.7 ± 2.5	2.4	15.1 ± 1.1	3.0	16.1	11.7 ± 1.3	8.2	35.1 ± 2.0	–	29.0	14.2 ± 0.9	–	10.7	–	–	–
H33S	25.0	13.9	22.3	17.2	14.7	41.9	0.0	35.0	32.7 ± 3.2	3.2	11.5 ± 1.3	2.7	12.2	7.7 ± 0.9	5.8	27.4 ± 1.1	–	29.4	8.5 ± 2.6	–	8.7	–	–	–
H33R	13.8	10.0	12.3	11.9	10.7	25.6	0.0	29.5	14.8 ± 1.7	2.4	7.6 ± 0.8	2.3	8.7	5.3 ± 0.5	5.1	18.9 ± 1.8	–	23.8	5.1 ± 0.5	–	6.2	–	–	–
H34S	11.5	8.7	12.6	10.3	10.0	22.6	0.0	21.1	25.2 ± 0.9	0.0	7.4 ± 0.4	1.5	7.2	4.4 ± 0.3	3.8	12.9 ± 1.4	–	14.5	4.9 ± 0.7	–	5.3	–	–	–
H34R	9.8	6.5	9.5	6.9	6.6	21.5	0.0	13.7	18.5 ± 1.8	0.0	6.1 ± 0.2	0.9	7.0	2.7 ± 0.2	3.4	10.7 ± 1.1	–	11.1	2.3 ± 0.2	–	3.6	–	–	–
H35S	10.2	4.7	10.0	8.6	8.4	0.0	0.0	0.0	0.0	0.0	6.2 ± 0.8	1.2	5.4	–	2.5	0.0	–	0.0	0.0	–	–	–	–	–
H35R	5.9	4.7	5.6	7.2	4.6	0.0	0.0	0.0	0.0	0.0	4.1 ± 0.2	1.1	3.6	–	1.8	0.0	–	0.0	0.0	–	–	–	–	–
Total	678.8	411.6	665.7	549.3	488.7	1036.2	143.0	1035.7	921.3	179.5	392.9	107.0	401.6	266.9	256.5	829.4	–	906.3	293.1	–	334.5	21.2	–	–
Steranes																								
S21	11.2	9.8	14.1	13.7	12.0	35.3	10.5	31.1	29.9 ± 2.9	16.3	11.7 ± 0.6	4.7	14.4	16.1 ± 1.5	10.4	36.7 ± 1.7	–	30.5	12.2 ± 1.7	–	15.3	4.9	1.1	0.0
S22	7.1	4.9	9.1	8.4	6.9	20.9	5.6	20.2	18.1 ± 1.1	9.1	6.3 ± 0.6	1.9	8.0	7.1 ± 1.1	5.1	17.5 ± 1.3	–	17.5	7.5 ± 1	–	6.9	1.5	0.5	0.0
C27dβαS	0.8	0.5	1.0	1.1	0.8	7.8	3.3	7.2	6.3 ± 0.5	2.9	0.9 ± 0.2	0.4	1.1	1.1 ± 0.2	0.6	3.8 ± 0.1	–	4.7	1.9 ± 0.3	–	1.2	0.5	0.1	0.0
C27dβαR	0.5	0.4	0.5	0.6	0.5	4.4	1.3	3.6	4.2 ± 0.1	1.8	0.6 ± 0.1	0.2	0.6	0.8 ± 0.1	0.4	2.6 ± 0.1	–	3.8	0.7 ± 0.1	–	0.5	0.3	0.1	0.0
C27ααα S	5.0	3.1	5.1	4.7	3.9	13.5	2.2	11.3	10.6 ± 0.8	3.0	4.1 ± 0.1	1.1	4.3	3.6 ± 0.2	2.8	10.4 ± 0.4	–	10.8	4.1 ± 0.3	–	4.3	0.4	0.2	0.1
C27αββR+29dβαS	5.6	3.1	5.9	5.3	4.3	16.9	2.6	15.0	13.7 ± 0.5	4.1	4.4 ± 0.3	1.3	4.7	4.3 ± 0.3	2.9	13.1 ± 0.2	–	13.7	4.4 ± 0.5	–	4.4	0.5	0.2	0.1
C27αββS	5.0	2.8	4.9	4.8	3.9	14.1	2.0	12.4	10.8 ± 0.7	3.3	3.7 ± 0.2	1.1	4.3	4.0 ± 0.1	2.5	10.2 ± 0.7	–	10.2	3.7 ± 0.1	–	4.1	0.4	0.2	0.0
C27αααR	5.3	2.6	5.0	4.5	3.8	15.5	2.6	12.8	11.6 ± 0.6	3.1	3.8 ± 0.1	0.9	4.2	3.9 ± 0.1	2.3	10.8 ± 1.1	–	10.7	3.9 ± 0.6	–	3.8	0.4	0.2	0.2
C28ααα S	2.8	1.5	2.7	2.7	1.9	7.0	1.2	6.4	4.8 ± 0.3	1.4	1.7 ± 0.2	0.6	2.1	2.0 ± 0.1	1.3	5.2 ± 0.2	–	5.2	1.9 ± 0.1	–	1.9	0.2	0.1	0.1
C28αββR	2.9	1.5	2.8	2.6	1.7	4.6	0.8	5.0	4.1 ± 0.1	1.0	1.6 ± 0.3	0.8	2.1	2.0 ± 0.2	1.3	3.6 ± 0.2	–	3.5	1.1 ± 0.1	–	1.9	0.3	0.1	0.0
C28αββS	3.0	1.8	3.0	2.3	1.7	5.7	1.3	7.1	5.8 ± 0.2	1.7	1.2 ± 0.2	0.6	1.8	1.6 ± 0.1	1.1	5.7 ± 0.1	–	6.2	2.1 ± 0.2	–	1.6	0.2	0.1	0.0
C28αααR	2.4	1.0	2.5	1.9	1.5	5.8	0.9	6.3	5.3 ± 0.1	1.0	1.4 ± 0.1	0.3	1.6	1.3 ± 0.1	0.9	4.3 ± 0.2	–	4.1	1.0 ± 0.3	–	1.3	0.1	0.1	0.1
C29ααα S	4.1	2.2	4.6	3.9	2.9	7.4	1.1	7.2	7.2 ± 0.3	1.4	2.6 ± 0.1	0.7	3.1	2.4 ± 0.2	1.6	6.4 ± 0.4	–	5.8	2.4 ± 0.2	–	2.5	0.2	0.1	0.1
C29αββR	4.6	2.6	5.0	4.1	3.5	12.3	1.4	12.3	10.4 ± 0.4	3.0	3.2 ± 0.2	0.8	3.3	3.0 ± 0.2	2.1	11.2 ± 0.4	–	9.7	3.0 ± 0.2	–	2.9	0.3	0.1	0.1
C29αββS	5.0	2.5	5.3	4.2	3.1	9.4	0.9	9.8	8.1 ± 0.3	2.1	2.9 ± 0.3	0.7	3.5	3.1 ± 0.1	1.7	7.6 ± 0.4	–	7.5	2.0 ± 0.3	–	2.6	0.3	0.1	0.1
C29αααR	4.3	1.8	4.1	3.2	3.1	9.2	0.9	9.2	7.6 ± 0.5	1.2	2.6 ± 0.1	0.5	3.0	2.4 ± 0.2	1.5	8.3 ± 0.3	–	7.2	2.3 ± 0.1	–	2.0	0.2	0.1	0.1

(*continued on next page*)

Table 4 (*continued*)

Biomarkers	300 °C										330 °C										350 °C			
	Anhydrous					Hydrous					Anhydrous						Hydrous				Anhydrous			
	N	S20	Fe1	Fe2	Fe3	N	S20	Fe1	Fe2	Fe3	N	S20	Fe1	Fe2	Fe3	N	S20	Fe1	Fe2	Fe3	N	S20	S50	S100
Total	69.6	42.3	73.4	67.9	55.4	189.7	38.6	176.9	150.4	56.5	52.7	16.7	61.9	58.7	38.5	157.4	–	151.0	54.2	–	57.4	10.7	3.6	1.0
Others																								
n-C17	254.1	252.0	240.4	254.1	262.7	286.1	282.0	274.1	275.8 ± 11.3	292.7	224.3 ± 2.9	204.2	222.0	208.1 ± 11.8	226.3	279.3 ± 8.2	–	292.3	191.4 ± 10.9	–	178.9	151.5	120.8	–
Pr	79.1	81.7	84.2	69.6	93.7	91.2	91.4	99.6	83.2 ± 4.1	105.3	69.1 ± 2.8	59.0	72.7	59.2 ± 2.9	67.4	87.1 ± 6.7	–	92.8	56.2 ± 4.2	–	45.3	37.3	31.5	–
n-C18	162.5	163.2	151.9	151.9	171.5	182.5	173.9	167.9	153.5 ± 7.8	192.5	135.4 ± 6.6	126.7	126.5	147.4 ± 5.2	138.6	166.5 ± 6.9	–	176.5	133.2 ± 7.2	–	113.3	114.3	88.2	–
Ph	86.9	96.1	100.6	86.8	97.2	106.9	113.2	117.2	92.6 ± 4.2	107.8	71.5 ± 2.6	63.8	73.6	76.1 ± 3.1	69.0	86.1 ± 1.2	–	91.4	67.8 ± 1.1	–	46.3	42.6	21.6	–

Note: "–" = undetected, N = Neat kerogen, S20 = 20% sulfur, S50 = 50% sulfur, S100 = 100% sulfur, Fe1 = FeS_2, Fe2 = $FeSO_4$, Fe3 = $Fe_2(SO_4)_3$.

Table 5
Molecular parameters for pyrolysates of bitumen at various experimental conditions.

Biomarker parameters	300 °C										330 °C										350 °C			
	Anhydrous					Hydrous					Anhydrous							Hydrous			Anhydrous			
	N	S20	Fe1	Fe2	Fe3	N	S20	Fe1	Fe2	Fe3	N	S20	Fe1	Fe2	Fe3	N	S20	Fe1	Fe2	Fe3	N	S20	S50	S100
C27/(C27 + C28 + C29)	0.44	0.48	0.45	0.47	0.45	0.51	0.59	0.45	0.47	0.58	0.48	0.50	0.48	0.50	0.49	0.48	–	0.49	0.55	–	0.53	0.50	0.46	0.49
C28/(C27 + C28 + C29)	0.20	0.19	0.18	0.20	0.18	0.19	0.21	0.22	0.21	0.19	0.19	0.19	0.18	0.17	0.19	0.18	–	0.19	0.16	–	0.19	0.21	0.22	0.22
C29/(C27 + C28 + C29)	0.36	0.33	0.37	0.33	0.37	0.30	0.20	0.32	0.32	0.23	0.33	0.31	0.34	0.33	0.32	0.34	–	0.33	0.30	–	0.28	0.29	0.32	0.29
(S21 + S22)/C_{27}–C_{29} regs	0.37	0.55	0.48	0.50	0.54	0.42	0.72	0.41	0.44	0.82	0.54	0.68	0.59	0.73	0.70	0.53	–	0.47	0.56	–	0.67	1.78	0.93	0.10
S21/S22	1.54	1.63	1.70	1.53	1.59	1.69	1.86	1.54	1.66	1.80	1.80	2.52	1.80	1.98	1.79	2.04	–	1.74	1.83	–	3.36	2.21	2.08	1.12
C27 dβαR/C27αααR	0.09	0.15	0.10	0.13	0.13	0.28	0.49	0.28	0.36	0.57	0.14	0.24	0.14	0.21	0.17	0.22	–	0.35	0.18	–	0.13	0.76	0.35	0.11
C29-αββ/(αββ+ααα)	0.53	0.56	0.53	0.54	0.52	0.57	0.54	0.57	0.55	0.66	0.55	0.55	0.53	0.55	0.55	0.56	–	0.57	0.52	–	0.55	0.58	0.53	0.45
C29-20S/(20S + 20R)	0.50	0.52	0.52	0.53	0.47	0.44	0.46	0.44	0.46	0.46	0.49	0.51	0.51	0.50	0.49	0.42	–	0.44	0.47	–	0.51	0.48	0.48	0.49
C23/(C23 + C24t)	0.59	0.61	0.60	0.59	0.59	0.60	0.66	0.57	0.59	0.61	0.60	0.62	0.61	0.60	0.61	0.61	–	0.61	0.55	–	0.59	0.63	–	–
Ts/(Ts + Tm)	0.18	0.20	0.16	0.18	0.18	0.19	0.31	0.20	0.19	0.22	0.18	0.25	0.17	0.15	0.21	0.16	–	0.16	0.20	–	0.20	0.29	–	–
C23/H30	0.23	0.31	0.24	0.28	0.30	0.27	0.73	0.22	0.24	0.79	0.34	0.44	0.35	0.44	0.45	0.25	–	0.24	0.33	–	0.54	1.10	–	–
H29/H30	0.92	0.99	0.87	0.90	0.97	0.97	1.05	0.94	0.95	1.03	1.08	1.10	1.07	0.97	1.09	0.99	–	0.97	1.07	–	1.27	1.31	–	–
H31-22S/(22S + 22R)	0.59	0.54	0.57	0.58	0.56	0.62	0.60	0.61	0.61	0.60	0.54	0.51	0.56	0.57	0.53	0.61	–	0.62	0.63	–	0.61	–	–	–
Gam/H30	0.03	0.05	0.03	0.03	0.04	0.13	0.21	0.08	0.07	0.21	0.03	0.04	0.03	0.05	0.03	0.10	–	0.27	0.95	–	0.04	–	–	–
Pr/*n*-C17	0.32	0.36	0.29	0.35	0.27	0.51	0.59	0.45	0.47	0.58	0.36	0.30	0.31	0.33	0.28	0.48	–	0.49	0.55	–	0.25	0.31	0.25	–
Ph/*n*-C18	0.56	0.57	0.54	0.66	0.57	0.19	0.21	0.22	0.21	0.19	0.55	0.50	0.53	0.58	0.52	0.18	–	0.19	0.16	–	0.37	0.52	0.41	–
Pr/Ph	0.89	0.96	0.68	0.84	0.80	0.30	0.20	0.32	0.32	0.23	0.95	0.98	0.91	0.99	0.78	0.34	–	0.33	0.30	–	0.88	0.96	0.98	–

Note: "–" = undetectable; S21-22/C_{27}–C_{29} regs: (diginane + 20-methyldiginane)/C_{27}–C_{29} regular steranes (12 peaks).

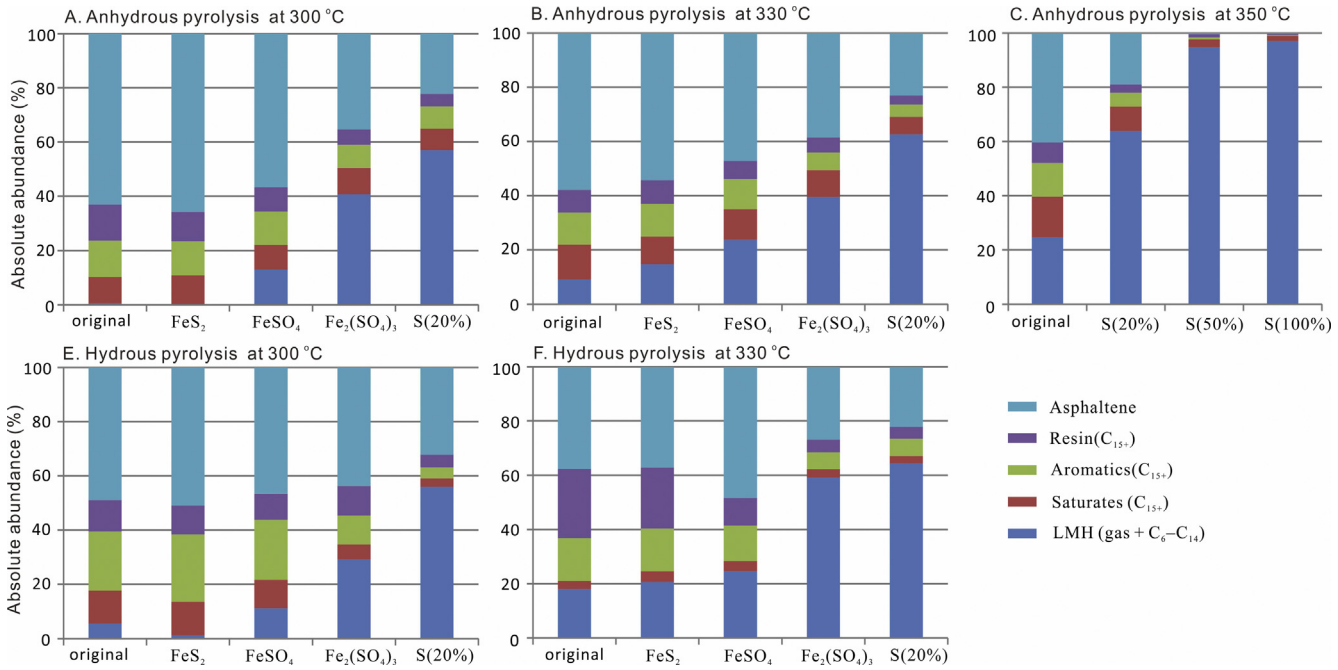

Fig. 2. The relative abundances of low molecular weight hydrocarbons (LMW, including gas and C_{6-14}), saturates, aromatics, resin and asphaltene fractions for pyrolysates of bitumen with various additives at different pyrolysis temperatures and conditions.

tetracyclic terpanes than those of the hopanes (Seifert and Moldowan, 1979; Trendel et al., 1982), apart from FeS_2 which had a negligible effect. Both $FeSO_4$ and $Fe_2(SO_4)_3$ promoted the thermal cracking of the hopanes (Fig. 3E). The addition of S^0 led to the most significant decline in the hopane concentrations. With 300 °C hydrous pyrolysis, the RAVR values of tricyclic terpanes and hopanes for FeS_2 and $FeSO_4$ was <−25%, whereas for S^0 and $Fe_2(SO_4)_3$ it was <−75% (Fig. 3B and 3F).

Anhydrous 330 °C pyrolysis results were similar to those of the 300 °C pyrolysis, with tricyclic terpanes RAVR values <−25% on addition of the sulfur-bearing minerals (Fig. 3C). At the higher temperature, the effects of different additives, especially for S^0, on the hopane concentrations were enhanced (RAVR values to −75%). Under hydrous 330 °C condition, tricyclic terpanes (Fig. 3D) and hopanes (Fig. 3H) were only detected from the FeS_2, $FeSO_4$ and neat kerogen experiments. Meanwhile, the absolute RAVR values of tricyclic terpanes and hopanes for FeS_2 (<25%) were much lower than those for $FeSO_4$ (approximately 75%).

3.2.2. Steranes

The precursors for steranes in the geological samples are sterols in eukaryotic organisms (Mackenzie et al., 1982a; de Leeuw et al., 1989). During anhydrous pyrolysis at 300 °C and 330 °C, FeS_2 had minimal impact on sterane concentration (compared to bitumen alone), while $FeSO_4$ and $Fe_2(SO_4)_3$ slightly impacted, and S^0 significantly impacted sterane production (Fig. 4A and C). With hydrous pyrolysis at 300 °C, FeS_2 and $FeSO_4$ had minor impact compared to bitumen alone (RAVR close to 0), while $Fe_2(SO_4)_3$ and S^0 significantly reduced the concentrations of steranes (RAVR approximately −75%). After hydrous pyrolysis at 330 °C no steranes were detected in the experiments with $Fe_2(SO_4)_3$ and S^0 (Table 4), whilst they were reduced with FeS_2 (RAVR < −25%), and more so with $FeSO_4$ (RAVR < −75%) (Fig. 4D).

3.2.3. Triaromatic steroid hydrocarbons

Triaromatic steroid hydrocarbons (TAS) are considered to be the aromatization products of monoaromatic steroids at the early stages of hydrocarbon generation (Mackenzie et al., 1982a, 1982b; Abbott et al., 1984). The S-additives had a similar effect on the TAS concentration of anhydrous pyrolysis at both 300 °C and 330 °C. FeS_2 similarly had little impact on the concentrations of TAS compared to bitumen alone, with absolute RAVR values close to 0 (Fig. 5 and Table 6). $Fe_2(SO_4)_3$ caused a slight reduction in the concentrations of TAS and S^0 caused a much larger reduction (Fig. 5A). Unusually, the presence of $FeSO_4$ increased the absolute concentrations of TAS (RAVR > 25%). This was likely due to additional release of the biomarkers from aromatic, polar and asphaltene fractions at low stages of maturity (e.g., Bowden et al., 2006). It is also possible that $FeSO_4$ catalyzed the aromatization of regular or other steroids in the original bitumen. With hydrous pyrolysis at 300 °C, the different forms of sulfur had a similar effect on the concentrations of TAS compared to those observed under anhydrous conditions (Fig. 5B). At 330 °C, no TAS were detected in the experiments using $Fe_2(SO_4)_3$ (Fig. 5D).

3.2.4. Rankings and mechanisms

Generally speaking, biomarker concentrations decrease with increasing maturity as a result of thermal degradation (e.g., Mackenzie et al., 1985; Abbott et al., 1990; Bishop and Abbott, 1993; Farrimond et al., 1998). The above results show that various sulfur forms can promotes the thermal alteration of biomarkers, although their effects on the evolution of biomarker concentrations can differ. The extent to which different forms of sulfur promoted thermal alteration of biomarkers was in the following order: S^0 > $Fe_2(SO_4)_3$ > $FeSO_4$ > FeS_2 (Figs. 3–5). This order is consistent with the effect of S-additives on bulk bitumen stability (Fig. 2). It is also consistent with the work by Lu et al (2012) who reported that hydrocarbons (pure n-C_{24}) reacted with S^0 (250 °C) at much lower temperatures than metal sulfates (430 °C for $MgSO_4$).

Bitumen is a very complex mixture of different sized hydrocarbons including many biomarkers. Previously observed effect of sulfur on OM may similarly relate to biomarkers. The free-radical mechanism suggests that the concentration of S radicals rather than bond strengths control the reaction rates of petroleum

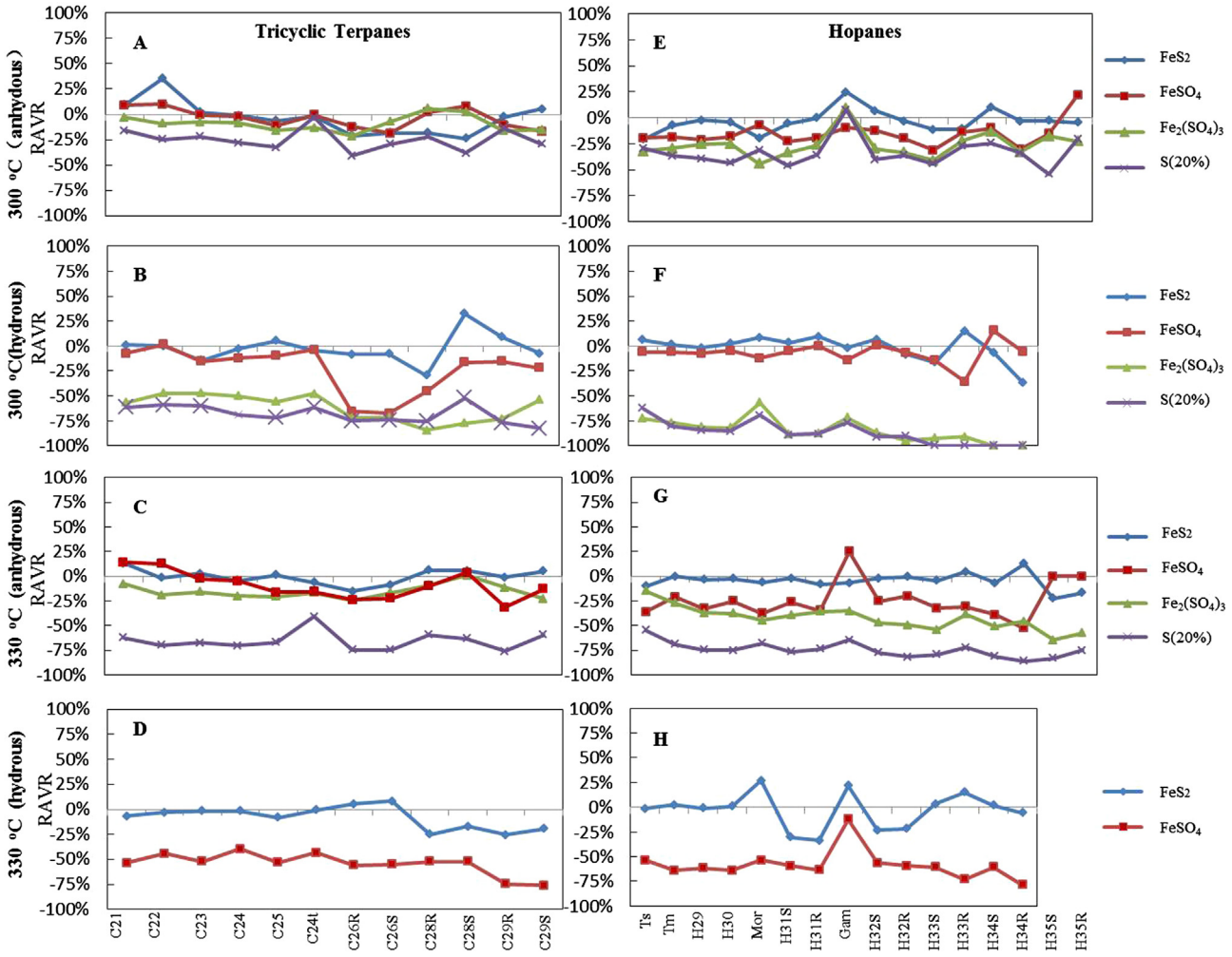

Fig. 3. The variations of RAVRs of terpane biomarkers in pyrolysates (under both the anhydrous and hydrous conditions) with various additives at 300 °C and 330 °C.

generation and evolution (Lewan, 1998). Specifically, the greater the concentration of initiating sulfur radicals formed in a reaction system of sedimentary organic matter, the higher the rate of organic matter thermal cracking. Under hydrous pyrolysis conditions, the generation temperature for sulfur radicals was above 150 °C for cyclo-S_8 allotropes (Goldstein and Aizenshtat, 1994); approximately 200 °C for the initiation of TSR by aqueous sulfate (Toland, 1960; Kiyosu and Krouse, 1993; Cross et al., 2004; Xia et al., 2014), and above 440 °C for the decomposition of pyrite (Levy and White, 1988). Under anhydrous conditions, cyclo-S_8 produced S-radical only above 175 °C (Goldstein and Aizenshtat, 1994), while pyrite decomposed to form the sulfur radical at temperatures >500 °C (Chen et al., 2000; Gai et al., 2014). The decomposition temperature of $Fe_2(SO_4)_3$ and $FeSO_4$ in a nitrogen atmosphere ranged from 550 °C to 625 °C (> the temperature used here), with decomposition products being Fe_2O_3 and FeO respectively (Siriwardane et al., 1999). However, our present experiments at 300 °C indicate ferrous and ferric sulfates have a catalytic effect on the pyrolysis of bitumen (Fig. 2), and possibly because the reducing gas (such as H_2S, H_2, CO, and CH_4) generated from the cracking of bitumen reduces the decomposition temperature of sulfate (Goldstein and Aizenshtat, 1994). Additionally, a small amount of water might also be present, and might also be thermally released from the polar fraction of bitumen. Thus, the anhydrous pyrolysis experiments with ferrous and ferric sulfate could include trace amounts of water. Therefore, the ease of generation of S-radicals from the S-additives was in the order S^0 > Fe(II)/Fe (III) sulfates > pyrite.

Furthermore, $Fe_2(SO_4)_3$ had a slightly stronger effect on the hydrocarbon reactant than $FeSO_4$ (Fig. 2), likely because of stronger Fe(III) reduction. Surdam and Crossey (1985) suggested that Fe(III) released during the transformation of smectite to illite may oxidize organic matter to produce organic acids. Seewald (2001; 2003) also noted that Fe(III) in sediments can oxidize hydrocarbons in subsurface environments. This may explain why $Fe_2(SO_4)_3$ has a stronger reduction effect on biomarkers than $FeSO_4$.

3.3. The influence of different forms of sulfur on biomarker parameters

3.3.1. Source-related biomarker parameters

The sterane ternary diagram for C_{27}–C_{29} 20R ααα-steranes is commonly used to correlate the source of oils and source rocks (Seifert et al., 1984; Seifert and Moldowan, 1986; Peters et al., 1989, 2005). Fig. 6 shows the distributions of C_{27}–C_{29} 20R ααα-steranes for the various S-additives at different pyrolysis temperatures and conditions. For the anhydrous experiments, bitumen alone and FeS_2 gave very similar distributions of C_{27}–C_{29} 20R ααα-steranes. The other additives produced only slight changes in the distributions (Fig. 6A).

However, with hydrous pyrolysis $Fe_2(SO_4)_3$ and S^0 significantly changed the distribution of the C_{27}–C_{29} 20R ααα-steranes at 300 °C and had removed all steranes at 330 °C (Table 5,

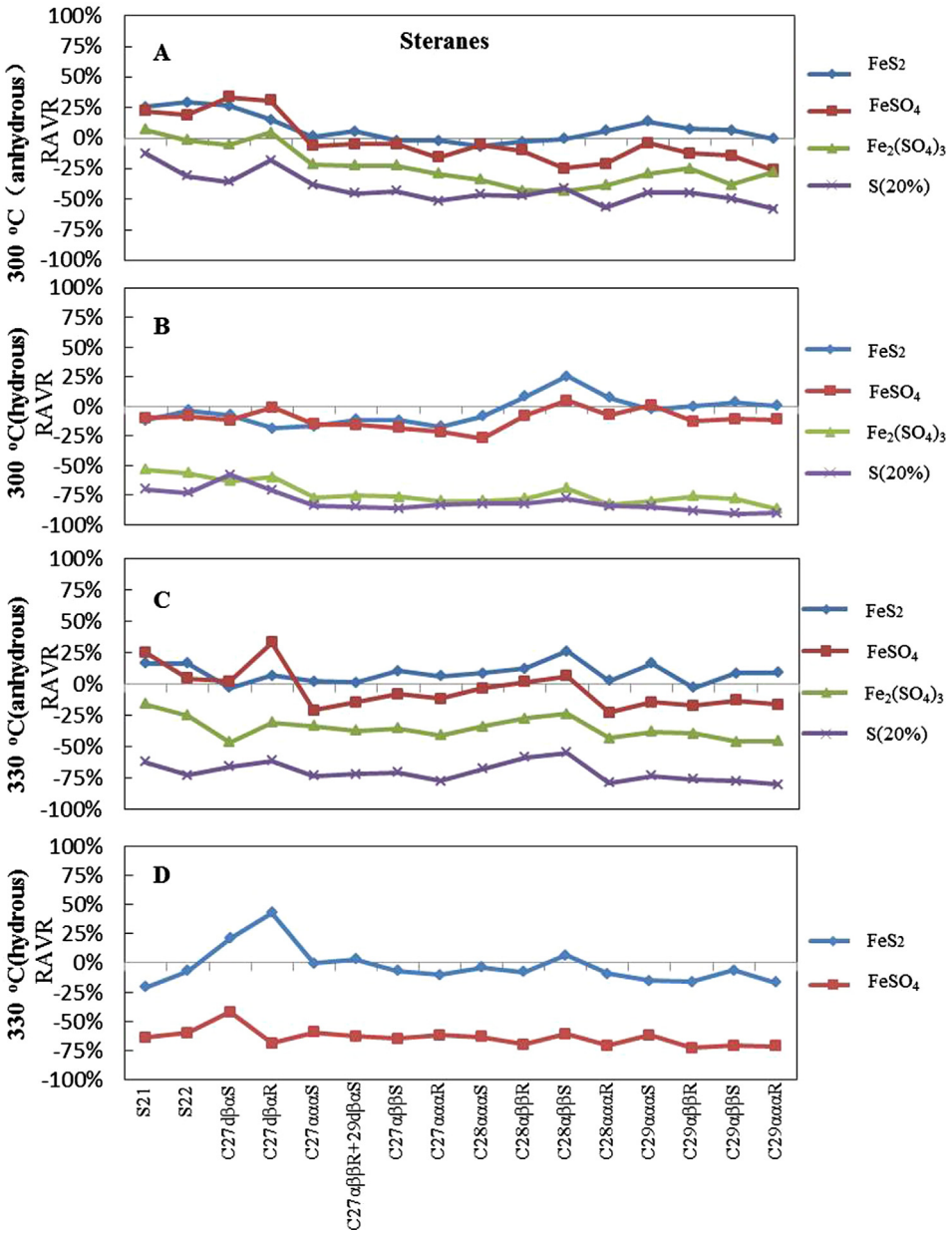

Fig. 4. The variations of RAVRs of sterane biomarkers in pyrolysates (under both the anhydrous and hydrous conditions) with various additives at 300 °C and 330 °C.

Fig. 4D). The steranes were also significate changed with $FeSO_4$ (compared to bitumen alone) at 330 °C (Fig. 6B). This indicates water enhances the influence that additives have on the thermal stability of steranes.

The ratio of diginane to 20-methyldiginane (S21/S22) is also widely used to correlate crude oils with potential source rocks (Huang et al., 1994; Fang et al., 2011; Wu et al., 2012). With anhydrous and hydrous pyrolysis at 300 °C, values of S21/S22 in the pyrolysates with sulfur-bearing minerals were quite stable (1.53–1.80; Table 5) and similar to the bitumen alone value (1.54). S^0 significantly changed the value of S21/S22 from 330 °C anhydrous pyrolysis and reduced the diginane to below detection limits with 330 °C hydrous pyrolysis (Fig. 7). $Fe_2(SO_4)_3$ similarly reduced diginane concentrations in the 330 °C hydrous pyrolysis.

Source-related biomarker parameters based on terpanes include the ratio of C_{29} 17α(H),21β(H)-hopane to C_{30} 17α(H),21β(H)-hopane (H29/H30), the ratio of C_{23} tricyclic terpane to C_{23} tricyclic terpane and C_{24} tetracyclic terpanes (C23/(C23 + C24t)), the ratio of gammacerane/C_{30} 17α(H),21β(H)-hopane (Gam/H30), and the ratio of tricyclic terpanes/17α-hopane (C23/H30) (Peters et al., 2005). These source-related biomarker parameters are based on the ratios of adjacent homologues or on compounds with similar structures and levels of thermal stability. The ratios of C23/(C23 + C24t), Gam/H30, and H29/H30 were not significantly changed by S-additives at 300 °C anhydrous or hydrous pyrolysis (Table 5 and Fig. 7). However, $Fe_2(SO_4)_3$ and S^0 added to 300 °C hydrous pyrolysis led to significantly higher C23/H30 values, and C23/H30 showed further variation between the different experiments (Fig. 7). The C23/H30 ratio is based on two biomarkers with quite different levels of thermal stability (Seifert and Moldowan, 1979; Peters et al., 2005), and thus is sensitive to differences in cracking reactions.

The distribution of TAS has also proved useful in determining the oil-to-source correlation between severely biodegraded oils

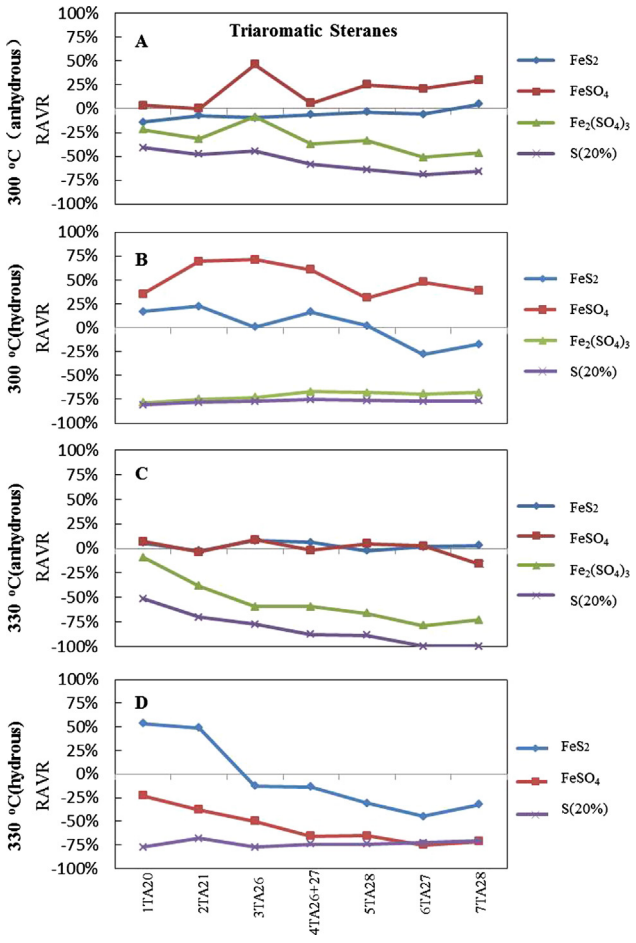

Fig. 5. The variations of RAVRs of triaromatic sterane biomarkers in pyrolysates (under both the anhydrous and hydrous conditions) with various additives at 300 °C and 330 °C.

and source rocks of similar thermal maturity (Peters et al., 2005). From Fig. 8, it is clear that the presence of elemental sulfur and sulfur-bearing minerals had negligible impact on the distribution of TAS under these pyrolysis conditions. This means that although the presence of elemental sulfur and sulfur-bearing minerals have significant effects on the absolute concentration of TAS (Fig. 5), they do not significantly change their relative distributions.

3.3.2. Maturity-related biomarker parameters

Most of the maturity-related biomarker parameters are based on hydrocarbon isomerization (rearrangement) or thermal cracking (including aromatization) reactions (Peters et al., 2005). Based on the isomerization of 17α-hopanes at C-22, the 22S/(22S + 22R) homohopane isomerization ratio for C_{31}–C_{35} hopanes is commonly used to access the thermal maturity of crude oil and source rocks (Peters et al., 2005). The C_{29} sterane isomer ratios of C29-ββ/(ββ+αα) and C29-20S/(20S + 20R) (the isomerization of regular steranes at C-20) also serve as useful maturity-related biomarker parameters. The rearrangement occurs only when the cleavage and renewed formation of bonds produces an inverted configuration relative to the starting asymmetric centre. Intramolecular rearrangements of hydrogen or alkyl groups can also form and are important for the formation of biomarkers such as diasteranes (rearranged steranes) and Ts (the rearranged product of Tm). The ratios of diasteranes/sterane and Ts/Tm are also commonly used for maturity assessments (McKirdy et al., 1983; Rullkötter et al., 1985). Here, the ratio of C_{27} cholestane to C_{27} diacholestane (C_{27}-βαR/C_{27}-ααR) for all pyrolysis experiments was calculated and compared as diasteranes/sterane ratio. Previous researchers have shown that diginane and 20-methyldiginane may originate from the thermal cracking of C_{27}–C_{29} regular steroids (Huang et al., 1994; Abbott et al., 1995). A recent work by Wang et al. (2015) further suggests that diginane, 20-methyldiginane and higher C_{23}–C_{26} 20-*n*-alkylpregnanes are the cracking products of steroids that are bound to kerogen. This means that the ratio of (diginane to 20-methyldiginane)/C_{27}–C_{29} regular steranes

Table 6
Absolute concentrations (μg/g) of aromatic biomarker from the pyrolysates of bitumen with various additives at different temperatures (anhydrous conditions).

Biomarkers	300 °C					330 °C					350 °C			
	N	S20	Fe1	Fe2	Fe3	N	S20	Fe1	Fe2	Fe3	N	S20	S50	S100
Phenanthrenes														
MP	164.7	199.1	184.0	171.7 ± 8.2	146.1	141.9 ± 8.1	124.5	126.2	159.4 ± 4.7	130.6	192.0	168.4	30.6	1.0
3-MP	68.9	70.3	62.8	60.1 ± 2.7	55.1	57.3 ± 3.3	44.0	51.4	52.7 ± 2.2	47.2	72.2	67.7	6.0	0.2
2-MP	57.3	59.9	61.1	53.9 ± 2.5	47.5	54.6 ± 3.5	40.4	45.4	55.4 ± 3.2	42.6	75.3	61.8	7.6	0.3
9-MP	139.1	148.6	155.2	146.3 ± 6.2	112.4	120.8 ± 7.9	89.8	113.1	120.7 ± 4.9	105.2	144.9	129.3	16.6	0.4
1-MP	84.6	100.0	89.3	81.3 ± 4.2	73.2	84.6 ± 4.4	57.7	69.3	86.7 ± 2.2	69.1	111.8	97.7	11.3	0.3
Total	514.7	577.9	552.4	513.3	434.3	471.5	356.4	405.3	481.1	394.7	596.3	524.9	72.1	2.2
Dibenzothiophenes														
DBT	377.3	383.0	302.8	321.3 ± 14.7	273.4	239.8 ± 9.20	235.1	247.1	281.2 ± 18.7	231.3	343.8	315.8	50.7	–
4-MDBT	249.0	280.3	248.0	245.4 ± 17.9	208.3	215.9 ± 8.4	173.2	179.3	212.6 ± 7.3	179.7	276.1	239.9	45.4	–
2,3-MDBT	200.4	209.2	208.8	178.9 ± 20.7	172.2	161.3 ± 6.5	136.5	140.0	148.3 ± 11.9	134.8	208.9	200.2	24.6	–
1-MDBT	124.5	152.1	129.5	120.5 ± 3.9	108.5	100.2 ± 3.1	91.6	90.1	105.6 ± 6.5	86.1	138.3	129.3	25.5	–
Total	951.2	1024.6	889.2	866.1	762.4	727.2	636.4	656.5	780.4	631.9	967.1	885.2	146.2	0.0
Triaromatic Steranes														
1TA20	4.2	4.7	5.4	6.4 ± 0.2	4.5	3.0 ± 0.2	1.6	3.4	3.4 ± 0.1	3.0	–	–	–	–
2TA21	3.3	3.3	4.7	4.7 ± 0.3	3.2	1.9 ± 0.1	0.6	2.0	1.9 ± 0.1	1.2	–	–	–	–
3TA26	0.6	0.6	0.7	1.0 ± 0.2	0.7	0.2 ± 0.1	0.0	0.3	0.2 ± 0.1	0.1	–	–	–	–
4TA26 + 27	1.7	1.3	2.3	2.2 ± 0.4	1.4	0.4 ± 0.1	0.1	0.6	0.4 ± 0.1	0.2	–	–	–	–
5TA28	1.5	0.9	2.0	2.3 ± 0.3	1.3	0.4 ± 0.1	0.0	0.5	0.4 ± 0.1	0.1	–	–	–	–
6TA27	0.9	0.5	1.3	1.5 ± 0.1	0.6	0.2 ± 0.1	–	0.2	0.2 ± 0.1	0.0	–	–	–	–
7TA28	1.3	0.7	1.7	1.9 ± 0.2	0.8	0.2 ± 0.1	–	0.3	0.2 ± 0.1	0.1	–	–	–	–
Total	13.6	12.0	18.2	20.0	12.4	6.3 ± 0.4	2.3	7.3	6.6 ± 0.3	4.7	0.0	0.0	0.0	0.0

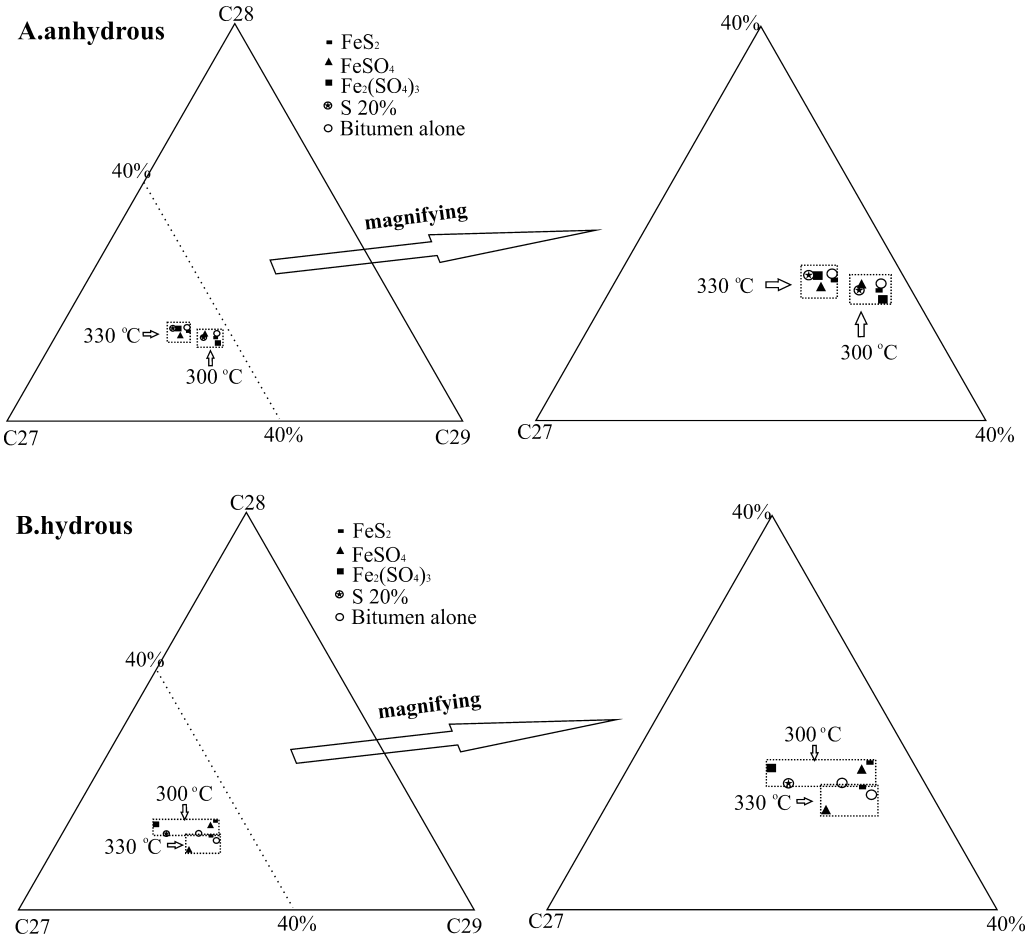

Fig. 6. Sterane ternary diagram of C_{27}–C_{29} 20R ααα-steranes in the pyrolysates (under both the anhydrous and hydrous conditions) with various additives at various temperatures.

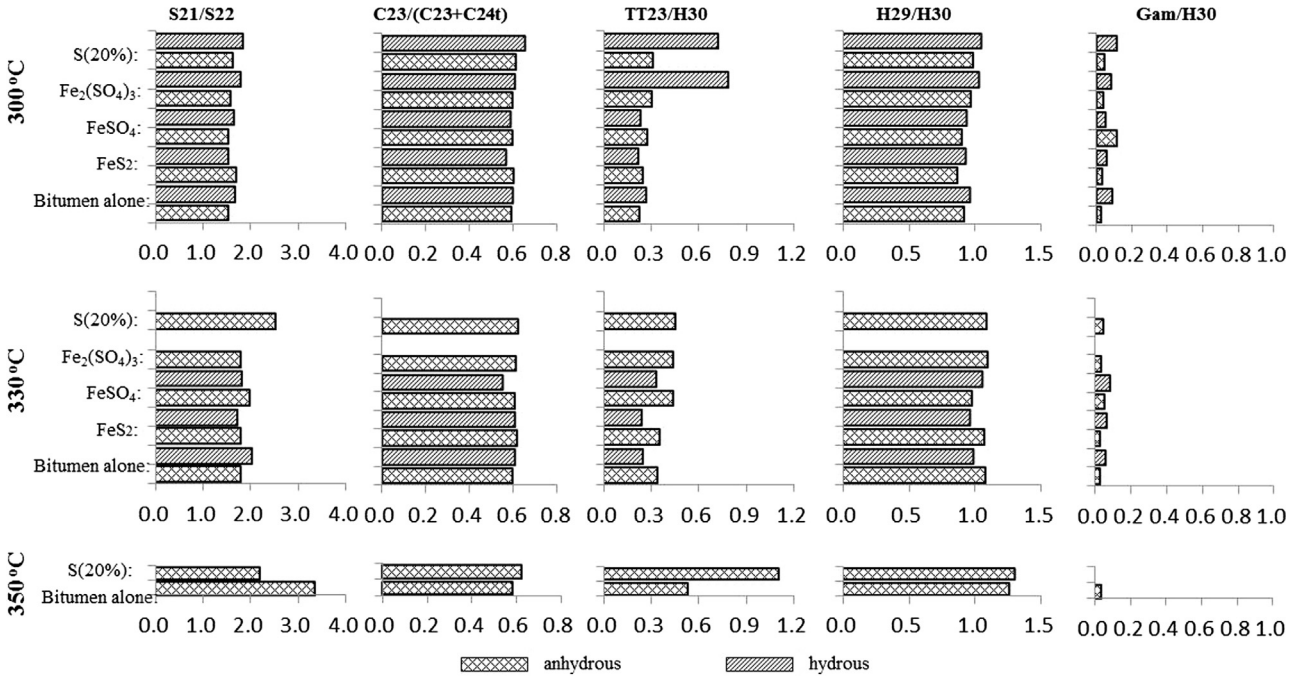

Fig. 7. Comparison of source-related biomarker parameters based on saturated hydrocarbons in the thermal altered bitumens plus various additives at different temperatures (under both the anhydrous and hydrous conditions).

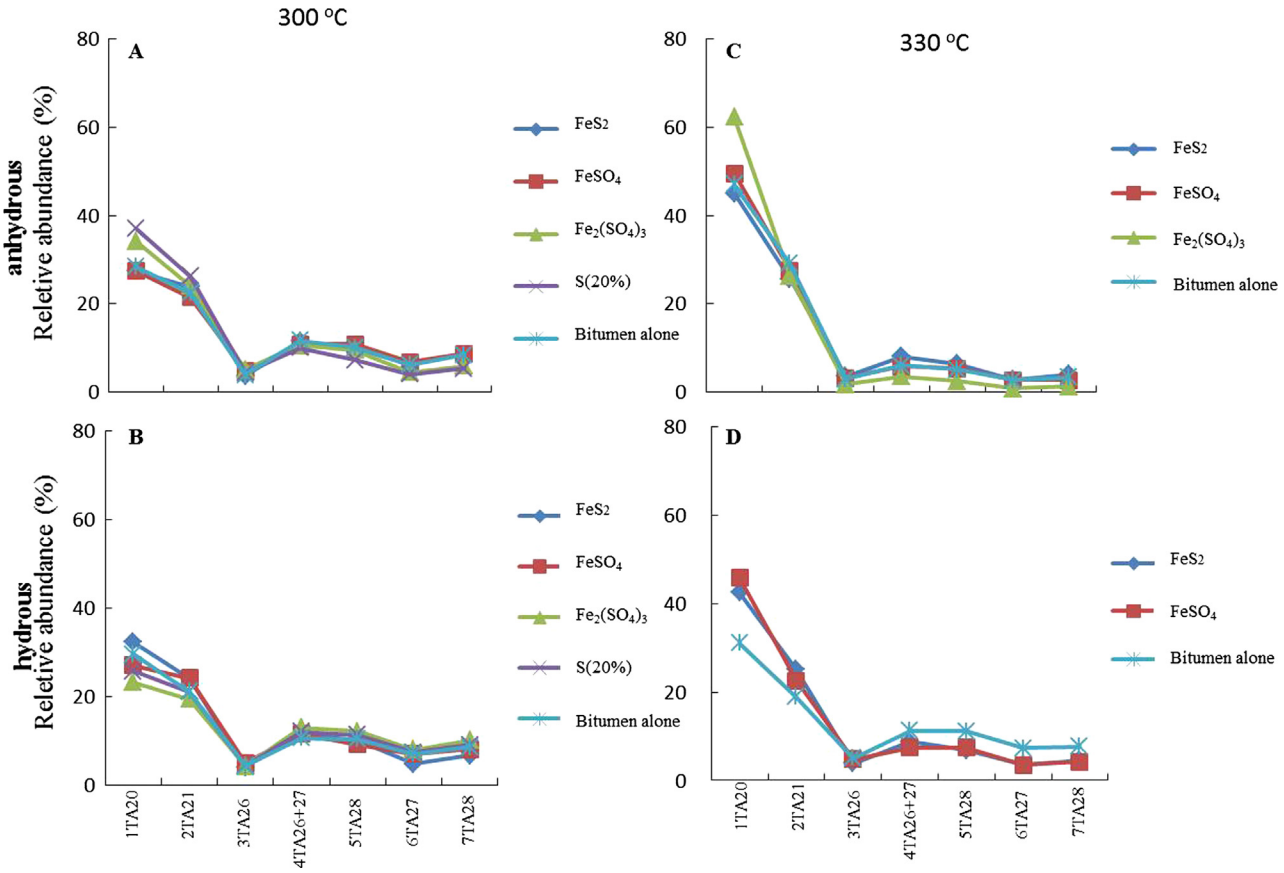

Fig. 8. The distribution of triaromatic steroid biomarkers in thermally altered bitumens plus different additives at various temperatures (under both anhydrous and hydrous conditions).

(12 peaks) ((S21 + S22)/C_{27}–C_{29} regs) may reflect the cracking of regular steranes.

Fig. 9 compares the maturity-related biomarker parameters of several sterane and hopane hydrocarbons obtained with the different S-additives and at different pyrolysis temperatures and H_2O. The S-additives had little effect on the isomerization ratios (C29-ββ/(ββ+αα), C29-20S/(20S + 20R), and H31-22S/(22S + 22R)) (Fig. 9), but, the presence of water did lead to consistently changed values. For example, the ratio of C29-20S/(20S + 20R) ranged from 0.47 to 0.53 for all of the anhydrous experiments conducted at 300 °C but reduced to 0.44 to 0.46 for the hydrous experiments conducted at 300 °C (Table 5 and Fig. 9).

The ratios of (S21 + S22)/C_{27}–C_{29} regs, C27dβαR/C27αααR, and Ts/Tm did show some variance with the different S-additives (Fig. 9). These three ratios presented very similar trends of evolution. (S21 + S22)/C_{27}–C_{29} regs, from anhydrous 300 °C pyrolysis was 0.37, but it increased to 0.48 to 0.55 with addition of the sulfur-bearing minerals (Table 5 and Fig. 9). At 330 °C, the S-additives had a greater effect. Anhydrous 330 °C values of (S21 + S22)/C_{27}–C_{29}regs for bitumen alone was 0.54, which sharply increased to 0.59 to 0.73 when sulfur-bearing minerals were present. A similar trend was observed with hydrous pyrolysis, which at 300 °C gave (S21 + S22)/C_{27}–C_{29} regs values which ranged from 0.42 to 0.82 (compared to 0.37 to 0.55 for anhydrous conditions). Meanwhile, all maturity-related biomarker parameters could not be calculated from our hydrous pyrolysis experiments of $Fe_2(SO_4)_3$ and S^0 at 330 °C. The general degradation of these products with hydrous 330 °C pyrolysis prevented the calculation of many of the biomarker ratios shown in Fig. 9.

In summary, at anhydrous and hydrous pyrolysis temperatures of 300 °C (Easy Ro: 0.70%), pyrite, the form of sulfur commonly found in source rocks, had almost no effect on the evolution of thermally sensitive biomarkers. On the other hand, the presence of SO_4^{2-} ($FeSO_4$ and $Fe_2(SO_4)_3$) and S^0 changed the source-related and maturity-related biomarker concentration and their distributions. The extent of the biomarker degradation was sensitive to the S-additives and the presence or not of H_2O. Under anhydrous conditions, elemental sulfur and metal sulfate had little effect at low thermal maturity stages (Easy Ro < 0.87%, pyrolysis temperature = 300 °C). When the Easy Ro reached 0.87% (330 °C pyrolysis), elemental sulfur and metal sulfate had a significant effect on relative biomarker abundance, yet some biomarker parameters still proved useful for oil-source correlations (e.g., C23/(C23 + C24t), H29/H30, Gam/H30 and TAS biomarkers). With water being present, elemental sulfur and metal sulfate had a significant effect on the evolution of these biomarkers even at the beginning of oil generative window (Easy Ro = 0.7%) and continued to influence their distributions to quite high maturities.

3.4. Geological significance

The applications of biomarkers to organic geochemistry are based on the principle that certain characteristics of biomarkers in migrated oil (reservoir stratum) do not differ significantly from remaining bitumen in the potential source rock and most source-related biomarker parameters are very stable in oil generative windows. This study further shows that the biomarker characteristics of source rocks may be altered by co-occurring sulfur and metal sulfates in oil generative windows. Although pyrite was only found to have a minor influence on the thermal evolution of the biomarkers, elemental sulfur and metal sulfate both significantly altered the bio-

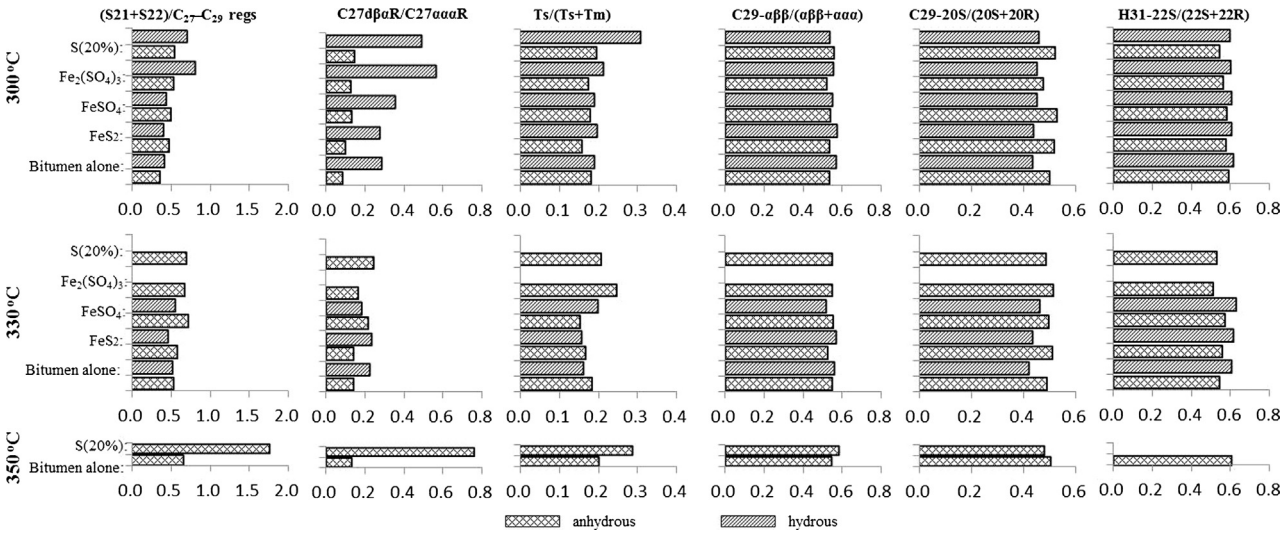

Fig. 9. Comparison of maturity-related biomarker parameters based on the saturated hydrocarbons in the thermally altered bitumens plus various additives at different temperatures (under both anhydrous and hydrous conditions).

marker concentrations and distributions obtained during pyrolysis at 300–350 °C (in the oil generative window). The presence of elemental sulfur in kerogen has previously been shown to significantly alter the thermally generated biomarkers from kerogen (Abbott et al., 1985; Comet et al., 1986, Wu and Geng, 2016). This emphasizes the importance of conducting oil-source rock correlations on oil samples and source rocks of similar thermal maturity and free of mineral influences. However, in many cases, available source rock candidates are of either higher or lower maturity than the oil sample. Hydrous pyrolysis (Lewan, 1985; Lewan et al., 1986) has been used to artificially increase the maturity of immature rocks (e.g., Peters et al., 1990; Moldowan et al., 1992).

Our current data has showed the catalytic effects of different forms of sulfur on the thermal evolution of biomarkers can be quite significant during hydrous (and anhydrous) pyrolysis at 300–350 °C which is equivalent to the oil generative window. This effect can increase with the relative abundance (compared to TOC) of sulfur-bearing minerals or elemental sulfur. Geological conditions of sulfur-bearing minerals can vary over a wide range and thus their impact on the hydrocarbon biomarker composition of sedimentary OM will also vary widely. Clay minerals and carbonate can also catalyze the physiochemical reaction of biomarkers in sediments during the diagenesis and catagenesis stages (e.g., Tannenbaum and Kaplan, 1985; Huizinga et al., 1987a,1987b; Lu et al., 1989; Jovančićević et al., 1992; Koopmans et al., 1998; Pan et al., 2009). Therefore, the pyrolysis of bulk source rock powders is considered to be more representative than the pyrolysis of kerogen, as it will include the influence of the mineral compositions (both clay minerals and sulfur-bearing minerals).

Many pyrolysis studies have investigated the kinetics of thermal evolution of organic matter (e.g., Lewan et al., 1986; Lu et al., 1989; Lewan, 1997; Liao et al., 2012; Wu and Geng, 2016), but few of these studies have considered the effect of clay minerals or sulfur-bearing minerals which may cohabit with sedimentary rocks. Most kerogen extractions isolate it from clay minerals and carbonates of the source rocks, so that subsequent kerogen analyses are free of mineral interference. However, sulfur and sulfur-bearing minerals may still exist in kerogen matrices obtained by normal acid treatment. Their removal may require more robust treatment such as heavy liquid separation (Nabbefeld et al., 2010; Holman et al., 2014), or chemical degradation with chromous chloride (Acholla and Orr, 1993), or sodium borohydride (Saxby, 1970).

4. Conclusions

The different effect of common sulfur-bearing compounds on the evolution of biomarkers in source rocks (bitumen) was measured by hydrous and anhydrous pyrolysis. The extent of the thermal alteration of biomarkers was ranked in the following order: S^0 > $Fe_2(SO_4)_3$ > $FeSO_4$ > FeS_2. FeS_2 had minimal effect on biomarker concentrations and distributions while SO_4^{2-} ($FeSO_4$ and $Fe_2(SO_4)_3$) and S^0 significantly reduced their concentrations, and changed their distributions generated during the oil maturity window. The product alterations are due to shifts in the radical mechanisms and TSR reactions.

Our results also show that the presence of water can significantly promote the alteration effects of the different sulfur forms. Under hydrous conditions (as in most common natural sedimentary environments), most source-related biomarker parameters varied with the presence of SO_4^{2-} ($FeSO_4$ and $Fe_2(SO_4)_3$) or S^0 even at the beginning of oil generative window (Easy Ro = 0.7%). Thus, reliable oil-source rock correlations should be conducted on samples of similar thermal maturity. If only an immature source rock candidate is available, the oil-source correlation based on the results from hydrous pyrolysis of source rock powders will be more reliable than the pyrolysis of kerogen. However, a kinetic investigation of kerogen free of S (i.e. with prior removal of elemental and mineral S) can facilitate the explanation of results.

This study focused on the effects of sulfur types on the thermal evolution of biomarkers in source rocks. Further study of the influence of different forms of sulfur on the thermal evolution of biomarkers in petroleum reservoirs will help to provide further knowledge of the role sulfur has on the geological fate of OM. The effect of gypsum, the dominant sulfur-bearing mineral associated with petroleum reservoirs will be of great relevance. The effect of sulfur-bearing minerals transported with migrated hydrocarbons from source rocks to reservoirs should also be considered.

Acknowledgements

This work was supported by the National Foundation of China (Grant Nos. 41673044 and 41303033), the National Science and Technology Major Project (Grant No. 2017ZX05008-002), and the Strategic Priority Research Program of the Chinese Academy of Sciences (Grant No. XDA14010101). This is contribution No. IS-

2551 from GIGCAS. We are grateful to Dr. Yankuan Tian for GC–MS analysis and laboratory assistance. Two anonymous reviewers are gratefully acknowledged for their constructive comments and suggestions. Special thanks go to the Associate Editor Dr. Paul Greenwood for the careful revision of the manuscript to improve its final English expression. We also thank Dr. John Volkman and Dr. Paul Greenwood for their great help and patience in handling the manuscript.

Associate Editor—**Paul Greenwood**

References

Abbott, G.D., Lewis, C.A., Maxwell, J.R., 1984. Laboratory simulation studies of steroid aromatization and alkane isomerization. Organic Geochemistry 6, 31–38.

Abbott, G.D., Lewis, C.A., Maxwell, J.R., 1985. Laboratory models for aromatization and isomerization of hydrocarbons in sedimentary basins. Nature 318, 651–653.

Abbott, G.D., Wang, G.Y., Eglinton, T.I., Home, A.K., Petch, G.S., 1990. The kinetics of sterane biological marker release and degradation processes during the hydrous pyrolysis of vitrinite kerogen. Geochimica et Cosmochimica Acta 54, 2451–2461.

Abbott, G.D., Bennett, B., Petch, G.S., 1995. The thermal degradation of 5α(H)-cholestane during closed-system pyrolysis. Geochimica et Cosmochimica Acta 59, 2259–2264.

Acholla, F.V., Orr, W.L., 1993. Pyrite removal from kerogen without altering organic matter: the chromous chloride method. Energy & Fuels 7, 406–410.

Amrani, A., Zhang, T.W., Ma, Q.S., Ellis, G.S., Tang, Y.C., 2008. The role of labile sulfur compounds in thermochemical sulfate reduction. Geochimica et Cosmochimica Acta 72, 2960–2972.

Bakr, M.Y., Yokono, T., Sanada, Y., Akiyama, M., 1991. Role of pyrite during the thermal degradation of kerogen using in situ high-temperature ESR technique. Energy & Fuels 5, 441–444.

Berner, R.A., 1989. Biogeochemical cycles of carbon and sulfur and their effect on atmospheric oxygen over Phanerozoic time. Palaeogeography Palaeoclimatology Palaeoecology 75, 97–122.

Berthonneau, J., Grauby, O., Abuhaikal, M., Pellenq, R.J.M., Ulm, F.J., Van Damme, H., 2016. Evolution of organo-clay composites with respect to thermal maturity in type II organic-rich source rocks. Geochimica et Cosmochimica Acta 195, 68–83.

Bishop, A.N., Abbott, G.D., 1993. The interrelationship of biological marker maturity parameters and molecular yields during contact metamorphism. Geochimica et Cosmochimica Acta 57, 3661–3668.

Bowden, S.A., Farrimond, P., Snape, C.E., Love, G.D., 2006. Compositional differences in biomarker constituents of the hydrocarbon, resin, asphaltene and kerogen fraction: an example from the Jet Rock (Yorkshire, UK). Organic Geochemistry 37, 369–383.

Cai, C.F., Worden, R.H., Bottrell, S.H., Wang, L.S., Yang, C.C., 2003. Thermochemical sulfate reduction and the generation of hydrogen sulfide and thiols (mercaptans) in Triassic carbonate reservoirs from the Sichuan Basin, China. Chemical Geology 202, 39–57.

Cai, C.F., Xie, Z.Y., Worden, R.H., Hu, G.Y., Wang, L.S., He, H., 2004. Methane dominated thermochemical sulphate reduction in the Triassic Feixianguan formation East Sichuan Basin, China: towards prediction of fatal H_2S concentrations. Marine and Petroleum Geology 21, 1265–1279.

Cai, C.F., Xiang, L., Yuan, Y.Y., Xu, C.L., He, W.X., Tang, Y.J., Borjigin, T., 2017. Sulfur and carbon isotopic compositions of the Permian to Triassic TSR and non-TSR altered solid bitumen and its parent source rock in NE Sichuan Basin. Organic Geochemistry 105, 1–12.

Chen, H.K., Li, B.Q., Zhang, B.J., 2000. Decomposition of pyrite and the interaction of pyrite with coal organic matric in pyrolysis and hydropyrolysis. Fuel 79, 1627–1631.

Chen, Z.H., Simoneit, B.R.T., Wang, T.G., Huang, W., Yan, D.T., Ni, Z.Y., Liu, K.Y., 2016. Effects of high temperatures on biomarker ratios during oil-to-gas cracking experiments at two pressures. Organic Geochemistry 101, 108–131.

Comet, P.A., McEvoy, J., Giger, W., Douglas, A.G., 1986. Hydrous and anhydrous pyrolysis of DSDP Leg 75 kerogens – a comparative study using a biological marker approach. Organic Geochemistry 9, 171–182.

Cross, M.M., Manning, D.A.C., Bottrell, S.H., Worden, R.H., 2004. Thermochemical sulphate reduction (TSR): experimental determination of reaction kinetics and implications of the observed reaction rates for petroleum reservoirs. Organic Geochemistry 35, 393–404.

de Leeuw, J.W., Cox, H.C., van Grass, G., van de Meer, F.W., Peakman, T.M., Baas, J.M. A., van de Graaf, V., 1989. Limited double bond isomerization and selective hydrogenation of sterenes during early diagenesis. Geochimica et Cosmochimica Acta 53, 903–909.

Ding, K.L., Liu, Y., 2017. Hydrolysis of pyrite: a possible pathway for generation of high concentrations of H_2S gas in deep-buried reservoirs? Development in Earth Science 5, 1–8.

Fang, Y.X., Liao, Y.H., Wu, L.L., Geng, A.S., 2011. Oil-source correlation for the paleo-reservoir in the Majiang area and remnant reservoir in the Kaili area, South China. Journal of Asian Earth Sciences 41, 147–158.

Farrimond, P., Taylor, A., Telnæs, N., 1998. Biomarker maturity parameters: the role of generation and thermal degradation. Organic Geochemistry 29, 1181–1197.

Francois, R., 1987. A study of sulfur enrichment in the humic fraction of marine-sediments during early diagenesis. Geochimica et Cosmochimica Acta 51, 17–27.

Gai, R.H., Jin, L.J., Zhang, J.B., Wang, J.Y., Hu, H.Q., 2014. Effect of inherent and additional pyrite on the pyrolysis behavior of oil shale. Journal of Analytical and Applied Pyrolysis 105, 342–347.

Garg, D., Givens, E.N., 1982. Pyrite catalysis in coal liquefaction. Industrial & Engineering Chemistry Process Design & Development 21, 113–117.

Goldhaber, M.B., Kaplan, I.R., 1975. Controls and consequences of sulfate reduction rates in recent marine sediments. Soil Science 119, 42–55.

Goldstein, T.P., Aizenshtat, Z., 1994. Thermochemical sulfate reduction - a review. Journal of Thermal Analysis 42, 241–290.

Heydari, E., Moore, C.H., 1989. Burial diagenesis and thermochemical sulfate reduction, Smackover Formation, southeastern Mississippi salt basin. Geology 17, 1080–1084.

Holman, A., Grice, K., Jaraula, C.M.B., Schimmelmann, A., 2014. Bitumen II from the Paleoproterozoic *Here's Your Chance* Pb/Zn/Ag deposit: Implications for the analysis of depositional environment and thermal maturity of hydrothermally-altered sediments. Geochimica et Cosmochimica Acta 139, 98–109.

Huang, D.F., Zhang, D.J., Li, J.C., 1994. The origin of 4-methyl steranes and pregnanes from Tertiary strata in the Qaidam Basin, China. Organic Geochemistry 22, 343–348.

Huizinga, B.J., Tannenbaum, E., Kaplan, I.R., 1987a. The role of minerals in the thermal alteration of organic matter-III. Generation of bitumen in laboratory experiments. Organic Geochemistry 11, 591–612.

Huizinga, B.J., Tannenbaum, E., Kaplan, I.R., 1987b. The role of minerals in the thermal alteration of organic matter-IV. Generation of *n*-alkanes, acyclic isoprenoids, and alkanes. Geochimica et Cosmochimica Acta 51, 1083–1097.

Jensen, H.K.B., Connan, J., Bjorøy, M., Hall, K., Wold, S., 1998. Geoelf sulphur analyser: quantification of thermally extractable and pyrolysable organic and mineral sulphur in source rocks. Organic Geochemistry 28, 87–110.

Jiang, C.Q., Li, M.W., 2002. Bakken/Madison petroleum systems in the Canadian Williston Basin. Part 3: geochemical evidence for significant Bakken-derived oils in Madison Group reservoirs. Organic Geochemistry 33, 761–787.

Jovančićević, B., Vitorović, D., Šaban, M., Wehner, H., 1992. Evaluation of the effects of native minerals on the organic matter of Aleksinac oil shale based on the composition of free and bound bitumens. Organic Geochemistry 18, 511–519.

Kelemen, S.R., Afeworki, M., Gorbaty, M.L., Sansone, M., Kwiatek, P.J., Walters, C.C., Freund, H., Siskin, M., 2007. Direct characterization of kerogen by X-ray and Solid-State ^{13}C Nuclear magnetic resonance methods. Energy & Fuels 21, 1548–1561.

Kiyosu, Y., Krouse, H.R., 1993. Thermochemical reduction and sulfur isotopic behavior of sulfate by acetic acid in the presence of native sulfur. Geochemical Journal 27, 49–57.

Koopmans, M.P., Carson, F.C., Sinninghe Damsté, J.S., Lewan, M.D., 1998. Biomarker generation from Type II-S kerogens in claystone and limestone during hydrous and anhydrous pyrolysis. Organic Geochemistry 29, 1395–1402.

Kowalewski, I., Schaeffer, P., Adam, P., Dessort, D., Fafet, A., Carpentier, B., 2010. Formation of H_2S and sulfur-rich bitumen from a reservoired heavy oil in the presence of elemental sulfur. Organic Geochemistry 41, 951–958.

Krouse, H.R., Viau, C.A., Eliuk, L.S., Ueda, A., Halas, S., 1988. Chemical and isotopic evidence of thermochemical sulfate reduction by light hydrocarbon gases in deep carbonate reservoirs. Nature 333, 415–419.

Lambert Jr., J.M., 1982. Alternative interpretation of coal liquefaction catalysis by pyrite. Fuel 61, 777–778.

Levy, J.H., White, T.J., 1988. The reaction of pyrite with water vapour. Fuel 67, 1336–1339.

Lewan, M.D., 1985. Evaluation of petroleum generation by hydrous pyrolysis experimentation. Philosophical Transactions of the Royal Society of London, Series A 315, 123–134.

Lewan, M.D., Bjorøy, M., Dolcater, D.L., 1986. Effects of thermal maturation on steroid hydrocarbons as determined by hydrous pyrolysis of Phosphoria Retort Shale. Geochimica et Cosmochimica Acta 50, 1977–1987.

Lewan, M.D., 1997. Experiments on the role of water in petroleum formation. Geochimica et Cosmochimica Acta 61, 3691–3723.

Lewan, M.D., 1998. Sulfur-radical control on petroleum formation rates. Nature 391, 164–166.

Liao, Y.H., Fang, Y.X., Wu, L.L., Geng, A.S., Hsu, C.S., 2012. The characteristics of the biomarkers and $\delta^{13}C$ of *n*-alkanes released from thermally altered solid bitumens at various maturities by catalytic hydropyrolysis. Organic Geochemistry 46, 56–65.

Lu, H., Greenwood, P., Chen, T.S., Liu, J.Z., Peng, P.A., 2012. The separate production of H_2S from the thermal reaction of hydrocarbons with magnesium sulfate and sulfur: implications for thermal sulfate reduction. Applied Geochemistry 27, 96–105.

Lu, S.T., Ruth, E.R., Kaplan, I.R., 1989. Pyrolysis of kerogens in the absence and presence of montmorillonite-I. The generation, degradation and isomerization of steranes and triterpanes at 200 and 300 °C. Organic Geochemistry 14, 491–499.

Machel, H.G., Krouse, H.R., Sassen, R., 1995. Products and distinguishing criteria of bacterial and thermochemical sulfate reduction. Applied Geochemistry 8, 373–389.

Mackenzie, A.S., Brassell, S.C., Eglinton, G., Maxwell, J.R., 1982a. Chemical fossils: the geological fate of steroids. Science 217, 491–504.
Mackenzie, A.S., Lamb, N.A., Maxwell, J.R., 1982b. Steroid hydrocarbons and the thermal history of sediments. Nature 295, 223–226.
Mackenzie, A.S., Rullkötter, J., Welte, D.H., Mankiewicz, P., 1985. Reconstruction of oil formation and accumulation in North Slope, Alaska, using quantitative gas chromatography-mass spectrometry. In: Magoon, L.B., Claypool, G.E. (Eds.), Alaska North Slope Oil/Source Rock Correlation Study. American Association of Petroleum Geologists, Tulsa, pp. 319–377.
Mango, F.D., 1990. The origin of light cycloalkanes in petroleum. Geochimica et Cosmochimica Acta 54, 23–27.
Meshoulam, A., Ellis, G.S., Ahmad, W.S., Deev, A., Sessions, A.L., Tang, Y.C., Adkins, J. F., Liu, J.Z., Gilhooly III, W.P., Aizenshtat, Z., Amrani, A., 2016. Study of thermochemical sulfate reduction mechanism using compound specific sulfur isotope analysis. Geochimica et Cosmochimica Acta 188, 73–92.
Metecan, İ.H., Saglam, M., Yanık, J., Ballice, L., Yüksel, M., 1999. The effect of pyrite catalyst on the hydroliquefaction of Göynük (Turkey) oil shale in the presence of toluene. Fuel 78, 619–622.
McKirdy, D.M., Aldridge, A.K., Ypma, P.J.M., 1983. A geochemical comparison of some crude oils from Pre-Ordovician carbonate rocks. In: Bjorøy, M. (Ed.), Advances in Organic Geochemistry. J. Wiley and Sons, New York, pp. 99–107.
Moldowan, J.M., Sundararaman, P., Salvatori, T., Alajbeg, A., Gjukic, B., Lee, C.Y., Demaison, G.J., 1992. Source correlation and maturity assessment of select oils and rocks from the Central Adriatic Basin (Italy and Yugoslavia). In: Moldowan, J.M., Albrecht, P., Philp, R.P. (Eds.), Biological Markers in Sediments and Petroleum. Prentice Hall, Englewood Cliffs, N.J., pp. 370–401.
Nabbefeld, B., Grice, K., Schimmelmann, A., Summons, R.E., Troitszch, U., Twitchett, R.J., 2010. A comparison of thermal maturity parameters between freely extracted hydrocarbons (Bitumen I) and a second extract (Bitumen II) from within the kerogen matrix of Permian and Triassic sedimentary rocks. Organic Geochemistry 41, 78–87.
Orr, W.L., 1974. Changes in sulfur content and isotopic ratios of sulfur during petroleum maturation - study of Big Horn Basin Paleozoic oils. American Association of Petroleum Geologists Bulletin 50, 2295–2318.
Ourisson, G., Albrecht, P., Rohmer, M., 1982. Predictive microbial biochemistry - from molecular fossils to prokaryotic membranes. Trends in Biochemical Sciences 7, 236–239.
Pan, C.C., Geng, A.S., Zhong, N.N., Liu, J.Z., Yu, L.P., 2009. Kerogen pyrolysis in the presence and absence of water and minerals: amounts and compositions of bitumen and liquid hydrocarbons. Fuel 88, 909–919.
Pan, C.C., Geng, A.S., Zhong, N.N., Liu, J.Z., 2010. Kerogen pyrolysis in the presence and absence of water and minerals: steranes and triterpenoids. Fuel 89, 336–345.
Peters, K.E., Moldowan, J.M., Driscole, A.R., Demaison, G.J., 1989. Origin of Beatrice oil by co-sourcing from Devonian and Middle Jurassic source rocks, Inner Moray Firth, U.K. American Association of Petroleum Geologists Bulletin 73, 454–471.
Peters, K.E., Moldowan, J.M., Sundararaman, P., 1990. Effects of hydrous pyrolysis on biomarker thermal maturity parameters: monterey phosphatic siliceous members. Organic Geochemistry 15, 249–265.
Peters, K.E., Walters, C.C., Moldowan, J.M., 2005. The Biomarker Guide, Biomarkers and Isotopes in Petroleum Exploration and Earth History. Cambridge University Press, New York.
Price, L.C., 1993. Thermal stability of hydrocarbons in nature: Limits, evidence, characteristics, and possible controls. Geochimica et Cosmochimica Acta 57, 3261–3280.
Riedinger, N., Brunner, B., Krastel, S., Arnold, G.L., Wehrmann, L.M., Formolo, M.J., Beck, A., Bates, S.M., Henkel, S., Kasten, S., Lyons, T.W., 2017. Sulfur cycling in an iron oxide-dominated, dynamic marine depositional system: the Argentine continental margin. Frontiers in Earth Science 5, 1–19.
Rosenberg, Y.O., Meshoulam, A., Said-Ahmad, W., Shawar, L., Dror, G., Reznik, I.J., Feinstein, S., Amarani, A., 2017. Study of thermal maturation processes of sulfur-rich source rock using compound specific sulfur isotope analysis. Organic Geochemistry 112, 59–74.
Rullkötter, J., Spiro, B., Nissenbaum, A., 1985. Biological marker characteristics of oils and asphalts from carbonate source rocks in a rapidly subsiding graben, Dead Sea, Israel. Geochimica et Cosmochimica Acta 49, 1357–1370.
Said-Ahmad, W., Amrani, A., Aizenshtat, Z., 2013. The action of elemental sulfur plus water on 1-octene at low temperatures. Organic Geochemistry 59, 82–86.
Sassen, R., 1988. Geochemical and carbon isotopic studies of crude-oil destruction, bitumen precipitation, and sulfate reduction in the deep Smackover formation. Organic Geochemistry 12, 351–363.
Saxby, J.D., 1970. Isolation of kerogen in sediments by chemical methods. Chemical Geology 6, 173–184.
Seewald, J.S., 2001. Aqueous geochemistry of low molecular weight hydrocarbons at elevated temperatures and pressures: constraints from mineral buffered laboratory experiments. Geochimica et Cosmochimica Acta 65, 1641–1664.
Seewald, J.S., 2003. Organic-inorganic interactions in petroleum-producing sedimentary basins. Nature 426, 327–333.
Seifert, W.K., Moldowan, J.M., 1979. The effect of biodegradation on steranes and terpanes in crude oils. Geochimica et Cosmochimica Acta 43, 111–126.
Seifert, W.K., Moldowan, J.M., Demaison, G.J., 1984. Source correlation of biodegraded oils. Organic Geochemistry 6, 633–643.
Seifert, W.K., Moldowan, J.M., 1986. Use of biological markers in petroleum exploration. Methods in Geochemistry and Geophysics 24, 261–290.
Siebert, R.M., 1985. The origin of hydrogen sulfide, elemental sulfur, carbon dioxide, and nitrogen in reservoirs. In: Timing of Siliciclastic Diagenesis. Sixth Annual Research Conference, Gulf Coast Section, Austin, Texas, Society of Economic Paleontologists and Mineralogists Foundation, pp. 30–31.
Siriwardane, R.V., Poston Jr., J.A., Fisher, E.P., Shen, M.S., Miltz, A.L., 1999. Decomposition of the sulfates of copper, iron (II), iron (III), nickel, and zinc: XPS, SEM, DRIFTS, XRD, and TGA study. Applied Surface Science 152, 219–236.
Surdam, R.C., Crossey, L.J., 1985. Organic-inorganic reactions during progressive burial: Key to porosity and permeability enhancement and preservation. Philosophical Transactions of the Royal Society A Mathematical Physical & Engineering Sciences 315, 135–156.
Sweeney, J.J., Burnham, A.K., 1990. Evaluation of a simple method of vitrinite reflectance based on chemical kinetics. American Association of Petroleum Geologists Bulletin 74, 1559–1570.
Tannenbaum, E., Kaplan, I.R., 1985. Low-molecular-weight hydrocarbons generated during hydrous and dry pyrolysis of kerogen. Nature 317, 708–709.
Thomas, M.G., Padrick, T.D., Stohl, F.V., Stephens, H.P., 1982. Decomposition of pyrite under coal liquefaction conditions: a kinetic study. Fuel 61, 761–764.
Tissot, B.P., Welte, D.H., 1984. Petroleum Formation and Occurrence. Springer-Verlag.
Toland, W.G., Hagman, D.L., Wilkes, J.B., Brutschy, F.J., 1958. Oxidation of organic compounds with aqueous base and sulfur. Journal of the American Chemical Society 80, 5423–5427.
Toland, W.G., 1960. Oxidation of organic compounds with aqueous sulfate. Journal of the American Chemical Society 82, 1911–1916.
Trendel, J.M., Restle, A., Connan, J., Albrecht, P., 1982. Identification of a novel series of tetracyclic terpane hydrocarbons (C_{24}–C_{27}) in sediments and petroleums. Journal of the Chemical Society, Chemical Communications, 304–306.
van Aarssen, B.G.K., Bastow, T.P., Alexander, R., Kagi, R.I., 1999. Distributions of methylated naphthalenes in crude oils: indicators of maturity, biodegradation and mixing. Organic Geochemistry 30, 1213–1228.
Wang, G.L., Chang, X.C., Wang, T.G., Simoneit, B.R.T., 2015. Pregnanes as molecular indicators for depositional environments of sediments and petroleum source rocks. Organic Geochemistry 78, 110–120.
White, C.M., Douglas, L.J., Schmidt, C.E., Hackett, M., 1988. Formation of polycyclic thiophenes from reaction of selected polycyclic aromatic hydrocarbons with elemental sulfur and/or pyrite under mild conditions. Energy & Fuels 2, 220–223.
Worden, R.H., Smalley, P.C., Oxtoby, N.H., 1995. Gas souring by thermochemical sulfate reduction at 140 °C. American Association of Petroleum Geologists Bulletin 79, 854–863.
Wu, L.L., Liao, Y.H., Fang, Y.X., Geng, A.S., 2012. The study on the source of the oil seeps and bitumens in the Tianjingshan structure of the northern Longmen Mountain structure of Sichuan Basin, China. Marine and Petroleum Geology 37, 147–161.
Wu, L.L., Liao, Y.H., Fang, Y.X., Geng, A.S., 2013. The deference in biomarkers released by hydropyrolysis and by Soxhlet extract from source rocks of different maturities and its geological implications. Chinese Science Bulletin 58, 373–383.
Wu, L.L., Geng, A.S., 2016. Differences in thermal evolution of hopanes and steranes in free and bound phase. Organic Geochemistry 101, 38–48.
Xia, X.Y., Ellis, G.S., Ma, Q.S., Tang, Y.C., 2014. Compositional and stable carbon isotopic fractionation during non-autocatalytic thermochemical sulfate reduction by gaseous hydrocarbons. Geochimica et Cosmochimica Acta 139, 472–486.
Zhan, Z.W., Tian, Y.K., Zou, Y.R., Liao, Z.W., Peng, P.A., 2016. De-convoluting crude oil mixtures from Palaeozoic reservoirs in the Tabei Uplift, Tarim Basin, China. Organic Geochemistry 97, 78–94.
Zhang, T.W., Ellis, G.S., Walters, C.C., Kelemen, S.R., Wang, K.S., Tang, Y.C., 2008. Experimental diagnostic geochemical signatures of the extent of thermochemical sulfate reduction. Organic Geochemistry 39, 308–328.
Zhang, T.W., Ellis, G.S., Ma, Q.S., Amrani, A., Tang, Y.C., 2012. Kinetics of uncatalyzed thermochemical sulfate reduction by sulfur-free paraffin. Geochimica et Cosmochimica Acta 96, 1–17.
Zhang, Z.N., Liu, W.H., Xia, Y.Q., Tengger, Wang, Z.D., Gao, B., Zhang, D.W., Qiu, J.L., 2011. Qualitative and quantitative analysis of the monatomic sulfur from marine source rocks in northeast Sichuan Basin. Journal of Mineral Petrology 125, 90–95 (in Chinese with English Abstract).
Zhu, G.Y., Zhang, S.C., Huang, H.P., Liang, Y.B., Meng, S.C., Li, Y.G., 2011. Gas genetic type and origin of hydrogen sulfide in the Zhongba gas field of the western Sichuan Basin, China. Applied Geochemistry 26, 1261–1273.
Zopfi, J., Ferdelman, T.G., Fossing, H., 2004. Distribution and fate of sulfur intermediates – sulfite, tetrathionate, thiosulfate, and elemental sulfur – in marine sediments. Geological Society of America Special Paper 379, 97–116.
Zou, H.Y., Hao, F., Zhu, Y.M., Guo, T.L., Cai, X.Y., Li, P.P., Zhang, X.F., 2008. Source rocks for the giant Puguang gas field, Sichuan Basin: implication for petroleum exploration in marine sequences in South China. Acta Geological Sinica – English Edition 82, 477–486.